Redshift distances in modified flat Friedmann-Lemaître-Robertson-Walker spacetime containing $g_{00}(t)$

Steffen Haase[*1]

[*]Leipzig, Germany

Abstract

In the present paper we use a modified flat Friedmann-Lemaitre-Robertson-Walker metric containing $g_{00}(t)$ describing a spatially homogeneous and isotropic universe to derive the cosmological redshift distance in a way which differs from that which can be found in the general astrophysical literature.

Using the flat Friedmann-Lemaitre-Robertson-Walker metric the radial physical distance is described by $R(t) = a(t)r$. In this equation the radial co-moving coordinate is named r and the time-depending scale parameter is named a(t). We use the co-moving coordinate r_e (the subscript e indicates emission) describing the place of a galaxy which is emitting photons and r_a (the subscript a indicates absorption) describing the place of an observer within a different galaxy on which the photons - which were traveling thru the universe - are absorbed. Therefore the physical distance - the real way of light - is calculated by $D = a(t_0)r_a - a(t_e)r_e \equiv R_{0a} - R_{ee}$. Here means $a(t_0)$ the today's (t_0) scale parameter and $a(t_e)$ the scale parameter at the time t_e of emission of the photons. The physical distance D is therefore a difference of two different physical distances from an origin of coordinates being on r = 0.

Nobody can doubt this real travel way of light: The photons are emitted on a co-moving coordinate place r_e and are than traveling to the co-moving coordinate place r_a. During this traveling the time is moving from t_e to t_0 ($t_e \leq t_0$) and therefore the scale parameter is changing in the meantime from $a(t_e)$ to $a(t_0)$.

Using this right physical distance we calculate some different redshift distances and some relevant classical cosmological equations (effects) and compare these theoretical results with some measurements of astrophysics (quasars, SN Ia and black hole).

We get the today's Hubble parameter $H_{0a} \approx 65.2$ km/(s Mpc) as a main result. This value is a little smaller than the Hubble parameter $H_{0,Planck} \approx 67.66$ km/(s Mpc) resulting from Planck 2018 data.

Furthermore, we find for the radius of the so-called Friedmann sphere $R_{0a} \approx 2{,}586.94$ Mpc. This radius is not the maximum possible distance of seeing within an expanding universe. Photons, which were emitted at this distance, are not infinite red shifted.

The today's mass density of the Friedmann sphere results in $\rho_{0m} \approx 9.09 \times 10^{-30}$ g/cm^3. For the mass of the Friedmann sphere we get $M_{Fs} \approx 1.94 \times 10^{55}$ g.

The mass of black hole within the galaxy M87 has the value $M_{BH,M87} \approx 1.56 \times 10^{43}$ g. The redshift distance of this object is $D \approx 19.60$ Mpc but its today's distance is only $D_0 \approx 12.27$ Mpc. The radius of this black hole is $R_S \approx 1.498 \times 10^{-3}$ pc.

Key words: relativistic astrophysics, theoretical and observational cosmology, redshift, Hubble parameter, quasar, galaxy, M87, SN Ia, black hole, flat universe, Friedmann-Lemaitre-Robertson-Walker metric, general relativity

PACS NO:

[1] steffen_haase@vodafone.de

Contents:

0. Motivation ... 3

1. Solving **the Einstein equations** ... 4

1.1 Solving the main Friedmann equation ... 5
2 Derivation of cosmological relevant relations ... 6

2.1 Previews ... 6
2.2 Redshift-scale parameter relation ... 9
2.3 The redshift distance ... 10
2.4 Hubble parameter ... 14
2.5 The magnitude-redshift relation ... 15
2.6 The angular size-redshift relation ... 16
2.7 The number-redshift relation ... 16
3. Derivation of further physical redshift distances ... 17

4. Determination of the parameter values ... 22

4.1 Magnitude-redshift relation ... 23
4.2 Number-redshift relation ... 25
4.3 Angular size-redshift relation ... 27
4.4 Fixing of R_{0a} with the help of SN Ia ... 28
4.5 Calculation of all possible redshift distances for the SN Ia ... 30
4.5.1 Absolute values of redshift distances ... 30
4.5.2 Peculiare velocities of SN Ia ... 32
4.5.3 Real redshift distances of SN Ia ... 32
4.6 Evaluation of the data from the black hole in M87 ... 34
4.7 Maximum values known today: Galaxy UDFj-39546284 and Quasar J0313 ... 35
5 About the mass of Friedman sphere ... 36

6. Hubble parameter again ... 38

7. Concluding remarks ... 42

8. Appendices ... 42

8.1 Equations ... 42
8.2 Tables ... 47

0. Motivation

In a paper we published earlier on cosmology with flat spacetime {[11] or [12]}, we found the following equation for the redshift distance $D(z; R_{0a}, \beta_{0m})$

$$D(z;R_{0a},\beta_{0m})=\frac{R_{0a}}{(1+z)}\left[\frac{1}{\beta_{0m}}\left(1-\frac{1}{\sqrt{1+z}}\right)+z\right] \quad . \tag{1}$$

In this equation, z is the redshift, $R_{0a} = a_0 r_a$ is the present-day radius of what we call the Friedmann sphere (a present-day visibility horizon for any conceivable observer when the ordinary Friedmann-Lemaitre-Robertson-Walker metric is used), and β_{0m} is a parameter of the theory that links together some physical properties of the expanding universe:

$$\frac{1}{\beta_{0m}}=\frac{2c_0}{R_{0a}\sqrt{\frac{8\pi G\rho_{0m}}{3}}}=\frac{c_0}{V_0} \quad . \tag{2}$$

Here a_0 is the current scale parameter and r_a is the co-moving radial coordinate location of the observer, which always remains constant.
The fundamental property of Eq. (1) is that D(z) --> R_{0a} applies for z ---> ∞. This means a today's visibility horizon for every conceivable observer.
In Eq. (2), c_0 is the speed of light in a vacuum (always within this paper), G is Newton's gravitational constant and ρ_{0m} is the current density of matter (subscript m) without taking into account possible radiation within the universe.
The name for the parameter β_{0m} was chosen - based on the SRT - because it is a quotient of a velocity V_0 and c_0.

By comparing our theory with three different astrophysical measurements, we found $\beta_{0m} = 1$, which is why

$$V_0=R_{0a}\sqrt{\frac{2\pi G\rho_{0m}}{3}}=c_0 \tag{2a}$$

can be written. According to this theory, the speed V_0 today is just equal to the speed of light c_0. From our point of view, this is no coincidence: the current value of the radius R_{0a} of the Friedmann sphere in combination with the current density of matter ρ_{0m} within the Friedmann sphere obviously generate the current value of the speed of light.

Because the radius $R_a(t) = a(t)r_a$ of the Friedmann sphere changes with time, the velocity V(t) is not constant in time either. If $V(t_0) = c_0$ applies today, then the speed of light itself is obviously time-dependent.

With this justification, in this paper we trace the effects of $g_{00}(t) = a_0/a(t)$ in a correspondingly modified Friedmann-Lemaître-Robertson-Walker metric (mFLRWM) for flat space

$$ds^2 = g_{00}(t)c_0{}^2dt^2 - a(t)^2\,dr^2 - a(t)^2 r^2\left(d\vartheta^2 + \sin^2\vartheta\, d\varphi^2\right) \quad . \tag{3}$$

In this metric, $g_{00}(t)$ acts similar to a time-dependent speed of light, which may even have been infinite at the time of the Big Bang.

1. Solving the Einstein equations

The topical standard model of cosmology assumes the correctness of Einstein's field equations (EFE) containing the Einstein tensor $G_{\mu\nu}$, the energy-momentum tensor $T_{\mu\nu}$, the metric tensor $g_{\mu\nu}$ and the Newtonian constant G describing the interaction of gravitation

$$G_{\mu\nu} = \frac{8\pi G}{c_0{}^4} T_{\mu\nu} - \Lambda\, g_{\mu\nu} \tag{4}$$

and solves these equations with the help of the in general curved Friedmann-Lemaitre-Robertson-Walker metric (FLRWM)

$$ds^2 = c_0{}^2dt^2 - a^2(t)\left[\frac{dr^2}{1-\varepsilon r^2} + r^2(d\vartheta^2 + \sin^2\vartheta d\varphi^2)\right] \quad , \tag{5}$$

which is suitable for the description of a homogeneous and isotropic universe evolving over time.

Λ is the cosmological constant which will neglected by us because the real physical meaning of it is not known at this time.
Furthermore, the so-called ΛCDM standard model of cosmology is not able to describe the magnitude-redshift relation of quasars and the angular size-redshift relation of cosmic objects for big redshifts z.
The base of the ΛCDM standard cosmological model is the dealing with too few SN Ia for big redshifts, what means that these measurement values are statistical not sufficiently enough. Therefore, it is not a god idea to introduce a further arbitrary parameter - Λ - in the theory of cosmology.
The comparison of the redshift distance calculated without using Λ shows, that the insertion of this constant is not needed, because the magnitude-redshift relation of quasars and the angular size-redshift relation can be interpreted very much with the theory developed by us within this paper.

We will use the more comfortable form instead of Eq. (4)

$$R_{\mu\nu} = -\frac{8\pi G}{c_0^{\,4}}\left(T_{\mu\nu} - \frac{T}{2} g_{\mu\nu}\right) \tag{6}$$

for solving of the EFE within this paper. $R_{\mu\nu}$ stands for the Ricci tensor and T is the trace of the energy-momentum tensor.
In accordance with our motivation, we solve the EFE setting $\Lambda = 0$ and take the flat mFLRWM [Eq. (3)]

$$ds^2 = \frac{a_0}{a(t)} c_0^{\,2} dt^2 - a^2(t) dr^2 - a^2(t) r^2 \left(d\vartheta^2 + \sin^2\vartheta \, d\varphi^2\right) \quad . \tag{3a}$$

The solution found by solving the EFE is the single main Friedmann equation (FE)

$$\dot{a} = \sqrt{\frac{2GM_{Fs}a_0}{r_a^{\,3}}} \; \frac{1}{a} \quad . \tag{A21}$$

The time-dependent cosmological scale parameter was designated with a(t) and its time derivative with a point above. The parameter a_0 is today's scale parameter and r_a the co-moving radiale coordinate of the observer, which is a constant all the time. With M_{Fs} the Friedmann mass was named. We have neglected a possible pressure of matter P.

All equations used for solving the EFE are given in appendix named "7.1 Equations".

Within the specialist literature, the following equation defines the Hubble parameter that is of course in general time depend because of a(t):

$$H_{lit} = \frac{\dot{a}}{a} = \sqrt{\frac{2GM_{Fs}a_0}{r_a^{\,3}}} \; \frac{1}{a^2} \quad . \tag{7}$$

If we refer to the today's Hubble parameter, we get

$$H_{0,lit} = \frac{\dot{a}_0}{a_0} = \sqrt{\frac{2GM_{Fs}}{a_0^{\,3} r_a^{\,3}}} \quad . \tag{8}$$

1.1 Solving the main Friedmann equation

Integrating the main FE [Eq. (A21)] we find the simple solution

$$a(t) = \sqrt{2}\sqrt[4]{\frac{2GM_{Fs}a_0}{r_a^{\,3}}}\,t^{\frac{1}{2}} \quad . \tag{9}$$

We will use later the resulting interval of time dt

$$dt = \frac{a\,da}{\sqrt{\frac{2GM_{Fs}a_0}{r_a^{\,3}}}} \tag{10}$$

for calculating the redshift distance.

Using Eq. (9) we can rewrite the Eq. (8) referring to today to

$$H_{0,lit} = \frac{1}{2t_0} \qquad or \qquad t_0 = \frac{1}{2H_{0,lit}} = \frac{1}{2}t_{H_{0,lit}} \qquad with \qquad t_{H_{0,lit}} = \frac{1}{H_{0,lit}} \quad . \tag{11}$$

We see that the age of universe - t_0 - is half as big as the Hubble time $t_{H0,lit}$. This means at the same times that the Hubble time cannot be used directly as the age of universe. - Altogether, the Hubble parameter is a simple function of time t.

Furthermore, we find that the Hubble parameter is a function of the quotient a_0/a_e:

$$H_{e,lit}(a_0, a_e) = H_{0,lit}\frac{a_0^{\,2}}{a_e^{\,2}} \quad . \tag{12}$$

Due to the result found within the chapter 2.2, we get the dependence of the Hubble parameter from the redshift [see Eq. (25)]. If we insert this formula in Eq. (12) we find

$$H_{e,lit}(z) = H_{0,lit}\,(z+1)\sqrt[3]{z+1} \quad . \tag{13}$$

Therefore, the Hubble parameter is a non-linear function of redshift. It starts with $H_{0,lit}$ for z = 0 and grows with z endless. Therefore, it makes no sense to use bigger redshifts for evaluation of the Hubble parameter.

2 Derivation of cosmological relevant relations

2.1 Previews

From the requirement of homogeneity it follows that all extra-galactic objects remain at their co-moving coordinate location r in the course of the temporal development of the universe, i.e. the co-moving coordinate distance between randomly selected galaxies does not change over time, the galaxies rest in this co-moving coordinate system. For this reason, dr/dt = 0 applies to them.
This does not apply to the freely moving photons inside the universe: they detach themselves from a galaxy at a certain point in time at a certain co-moving coordinate location, and are then later absorbed at a completely different co-moving coordinate location.

Here we introduce the designation r_e (the subscript **e** indicates **e**mission of light) for the co-moving coordinate location of the light-emitting galaxy and name the co-moving coordinate location of the galaxy in which the observer resides r_a (the subscript **a** indicates **a**bsorption of light). In the Euclidean space considered here, both variables mark the co-moving coordinate distance from an origin of coordinates r = 0. The constant co-moving coordinate distance between the two galaxies is therefore calculated to be $r_a - r_e$ if we assume that the galaxy of the observer is more depart from the origin of coordinates as the light-emitting galaxy. The light should therefore move from the inside to the outside within a spherical assumed mass distribution (outgoing photons), which serves as a simple model for the universe (using the FLRWM, it is quite easy to arrange that all directions are of a radial kind).

Due to the measurable expansion of the universe we know that in the course of cosmic evolution all real physical distances R(t) = a(t)r over the time-dependent scale parameter a(t) being stretched according to the solution (9) of FE [Eq. (A21)].

For a galaxy resting in the coordinate system of the flat mFLRWM, the real physical distance from the origin of coordinates becomes calculated to

$$R(t) = a(t)\int_0^r d\bar{r} = a(t)\,r \quad . \tag{14}$$

The radial co-moving coordinate r does not depend on time for galaxies.

The physical distance of the light-emitting galaxy from the origin of coordinates at time t_e (the time at that time) is therefore

$$R_e(t_e) = a(t_e)\,r_e \equiv a_e r_e = R_{ee} \quad , \tag{15}$$

while for the analog distance of the galaxy containing the observer at the same time

$$R_a(t_e) = a(t_e)\,r_a \equiv a_e r_a = R_{ea} \tag{16}$$

applies. The physical distance of both galaxies at the time t_e is therefore

$$D(t_e) = D_e = a_e r_a - a_e r_e = a_e (r_a - r_e) = R_{ea} - R_{ee} \quad . \tag{17}$$

For the physical distance between both cosmic objects at a later time - means today‘s time here - $t_0 > t_e$ then applies

$$D(t_0) = D_0 = a_0 r_a - a_0 r_e = a_0 (r_a - r_e) = R_{0a} - R_{0e} \quad . \tag{18}$$

However, both distances mentioned above are worthless for the computation of cosmological relevant distance relations, since the emitted photons make their physical way to the observer, which has to be calculated in accordance with

$$D = a_0 r_a - a_e r_e = R_{0a} - R_{ee} \quad . \tag{19}$$

To see this, imagine a photon that detaches itself at the time $t_e < t_0$ from the emitting galaxy at the co-moving coordinate r_e, where the scale parameter at this time has the value a_e. After the photon has moved freely through the expanding universe, it will arrive at the co-moving coordinate point r_a, the place of the observer within another galaxy, at time t_0, with the scale parameter at that time being a_0. Thus, the photon does not travel the path described by Eq. (17) nor by Eq. (18). The real physical distance traveled by the photon is always unequal to any one of these two distances. This must be taken into account when deriving the redshift distance.

The real physical light path is illustrated by the green line in Fig. 1:

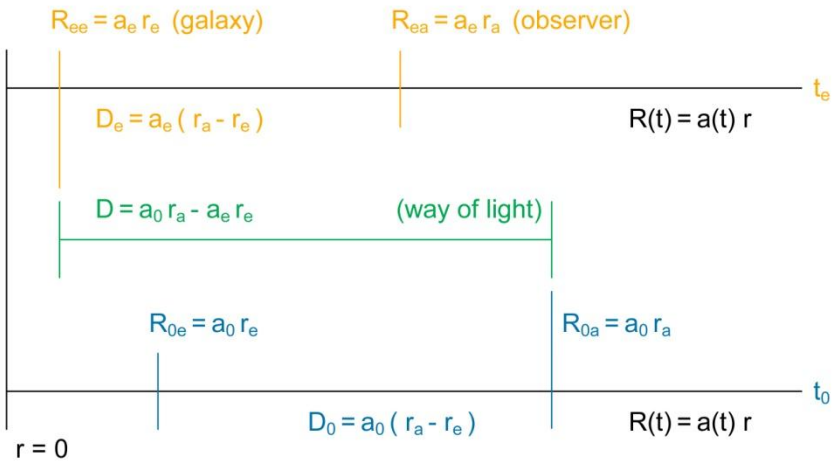

Figure 1. Real physical light path.

These remarks may be sufficient as a preliminary to the now following derivation of the redshift distance.

2.2 Redshift-scale parameter relation

For photons, ds = 0 and therefore

$$\int_{t_e}^{t_0} \frac{dt}{a\sqrt{a}} = \frac{1}{\sqrt{a_0}c_0} \int_{r_e}^{r_a} dr \quad . \tag{20}$$

This results in two light wave crests that are emitted in close succession,

$$\mathrm{X} = \int_{t_e}^{t_0} \frac{dt}{a\sqrt{a}} = \int_{t_e+\delta t_e}^{t_0+\delta t_0} \frac{dt}{a\sqrt{a}} \quad . \tag{21}$$

δt_0 is the distance in time between the two light wave crests on arrival at the observer and δt_e is the distance in time between the two light wave crests on emission.
Due to the very short time difference between the emission of the two light wave crests, both cover the same distance between the light source and the observer despite $da/dt \neq 0$. The integration therefore results in

$$0 = \frac{\delta t_0}{a_0\sqrt{a_0}} - \frac{\delta t_e}{a_e\sqrt{a_e}} \quad . \tag{22}$$

Let us arrange δt_0 and δt_e frequencies according to

$$\nu_0 = \frac{1}{\delta t_0} \qquad \textit{and} \qquad \nu_e = \frac{1}{\delta t_e} \qquad \textit{with} \qquad \nu_i = \frac{c_0}{\lambda_i} \quad . \tag{23}$$

So we get by means of

$$z = \frac{\lambda_0}{\lambda_e} - 1 \tag{24}$$

the desired redshift-scale parameter relation

$$\frac{a_0\sqrt{a_0}}{a_e\sqrt{a_e}} = (z+1) \qquad \textit{or} \qquad \frac{a_e}{a_0} = \frac{1}{(z+1)^{\frac{2}{3}}} \qquad \textit{or} \qquad a_0 = (z+1)^{\frac{2}{3}} a_e \quad . \tag{25a,b,c}$$

This relation is not the same relation how we can find for the not modified FLRWM.

2.3 The redshift distance

We now want to investigate which equation results for the redshift distance (corresponding to the photon path), which depends on the redshift z, if the integral

$$\int_{r_e}^{r_a} dr = +c_0\sqrt{a_0}\int_{t_e}^{t_0}\frac{dt}{a^{\frac{3}{2}}(t)} \tag{26}$$

is used. This integral results when our line element ds is set equal to zero in the mFLRWM [Eq. (3a)] and radial ($\vartheta = \varphi = \text{const}$) outgoing photons are considered. Eq. (26) describes the motion of photons inside the universe traveling from the co-moving coordinate r_e to the co-moving coordinate r_a.
During the travel time of the photons, the scale parameter changes from $a(t_e) = a_e$ to $a(t_0) = a_0$. If the time differential dt is replaced using Eq. (10), follows from Eq. (26)

$$\int_{r_e}^{r_a} dr = +c_0\sqrt{\frac{r_a^{\,3}}{2GM_{Fs}}}\int_{a_e}^{a_0} a^{-\frac{1}{2}}da \quad . \tag{27}$$

After executing of the integral we get

$$r_a - r_e = 2c_0\sqrt{\frac{r_a^{\,3}}{2GM_{Fs}}}\left(a_0^{\frac{1}{2}} - a_e^{\frac{1}{2}}\right) \quad . \tag{28}$$

Some further simple calculation steps result in

$$r_a - r_e = 2c_0\sqrt{\frac{r_a^{\,3}}{2GM_{Fs}}}a_0^{\frac{1}{2}}\left(1-\frac{a_e^{\frac{1}{2}}}{a_0^{\frac{1}{2}}}\right) = 2c_0\sqrt{\frac{a_0 r_a^{\,3}}{2GM_{Fs}}}\left(1-\sqrt{\frac{a_e}{a_0}}\right) \quad . \tag{29}$$

Now we multiply both sides with a_0 and get

$$a_0 r_a - a_0 r_e = 2c_0 a_0\sqrt{\frac{a_0 r_a^{\,3}}{2GM_{Fs}}}\left(1-\sqrt{\frac{a_e}{a_0}}\right) = 2c_0\sqrt{\frac{a_0^{\,3} r_a^{\,3}}{2GM_{Fs}}}\left(1-\sqrt{\frac{a_e}{a_0}}\right) \quad . \tag{30}$$

On the left side of Eq. (30) is not yet the real path traveled by the photon, but the today's physical distance $D_0 = a_0(r_a - r_e)$ of the two galaxies involved.

We now introduce the redshift. To this end, we take the relation between the two scale parameters a_e and a_0 at two different times t_e and t_0 how it was calculated to be Eq. (25a,b,c).

If Eq. (25c) and Eq. (25b) are inserted into Eq. (30), the result is

$$a_0 r_a - (z+1)^{\frac{2}{3}} a_e r_e = 2 c_0 \sqrt{\frac{{a_0}^3 {r_a}^3}{2GM_{Fs}}} \left(1 - \sqrt{\frac{1}{(z+1)^{\frac{2}{3}}}}\right) \quad . \tag{31}$$

Next, all unknown variables have to be eliminated from Eq. (31). Therefore we use the light path D introduced by Eq. (19)

$$a_e r_e = a_0 r_a - D = R_{0a} - D \tag{19a}$$

to find

$$D(z; R_{0a}, B_0) = \frac{R_{0a}}{(z+1)^{\frac{2}{3}}} \left\{ B_0 \left[1 - \frac{1}{(z+1)^{\frac{1}{3}}} \right] + (z+1)^{\frac{2}{3}} - 1 \right\} \quad . \tag{32}$$

This is the equation for the redshift distance, for which we were searching.

We have introduced the parameter B_0

$$B_0 = 2 c_0 \sqrt{\frac{R_{0a}}{2GM_{Fs}}} \qquad or \qquad B_0 = 2\sqrt{\frac{R_{0a}}{R_S}} \qquad with \qquad R_S = \frac{2GM_{Fs}}{{c_0}^2} \tag{33a,b,c}$$

as a further abbreviation.

R_S is a formal introduced Schwarzschild radius. It does not play the same role here in cosmology as it does within the Schwarzschild metric. $R_{0a} = a_0 r_a$ is the radius of the Friedmann sphere (Fs) so called by us, which contains the gravitational effective mass M_{Fs}.

The redshift distance D is therefore a function of z and the two parameters R_{0a} and B_0, which both can be determined fundamental by fitting the equation to appropriate astrophysical measurements.

The astrophysical literature does not know the parameter B_0. It results from the non-zeroing of r_a for the observer and of $r_e \neq 0$ for the observed galaxy, respectively.

For $B_0 = 1$ the following simple equation results

$$D(z; R_{0a}, B_0 = 1) = R_{0a} \left[1 + \frac{1}{(z+1)} \right] \quad . \tag{34}$$

The mass M_{Fs} takes into consideration all non-relativistic gravitational effective components within the Friedmann sphere: $M_{Fs} = \sum M_i$. These can also be different energy components E_i, to which, according to Einstein's energy-mass relationship $M_i = E_i/c^2$, masses M_i can be assigned.
In addition, with M_{Fs} as the total mass, such mass components that are invisible to us - perhaps only so far - are taken in to consideration.

Using R_S instead of B_0 we can rewrite the redshift distance as

$$D(z;R_{0a},B_0)=\frac{R_{0a}}{(z+1)^{\frac{2}{3}}}\left\{2\sqrt{\frac{R_{0a}}{R_S}}\left[1-\frac{1}{(z+1)^{\frac{1}{3}}}\right]+(z+1)^{\frac{2}{3}}-1\right\} \quad . \tag{35}$$

For $B_0 = \mathbf{2}$ we would get $R_{0a} = R_S$. In this case, we could believe that every observer is places (formally) on the surface of a black hole (corresponding to the Friedmann sphere) and that he always looks into a black hole while observing. Nevertheless, this is not a right thought because on the other side of each Friedmann sphere always matter exists.

We can interpret the parameter B_0 as a quotient of two velocities {how it was done in our former paper [11] or [12]}

$$B_0 = 2c_0\sqrt{\frac{R_{0a}}{2GM_{Fs}}} \equiv \frac{c_0}{V_0} \qquad or \qquad B_0 = 2\sqrt{\frac{R_{0a}}{R_S}} \equiv \frac{c_0}{V_0} \qquad or \qquad V_0 = \frac{c_0}{B_0} \quad . \tag{36a,b,c}$$

V_0 means $V(t_0)$. The velocity V(t) depends from time because $R_a(t)$ is also a function of time.
For $B_0 = 1$, $R_{0a} = R_S/4$ results and the speed V_0 would be exactly identical to the today's speed of light c_0.

If the comparison with the measurement data would real show $B_0 = 1$, we would get

$$D(z;R_{0a},B_0=1)=\frac{R_S}{4}\left[1-\frac{1}{(z+1)}\right] \quad . \tag{34a}$$

In this case, we would immediately see that the total mass M_{Fs} of the Friedmann sphere goes directly into the equation in form of the formally introduced Schwarzschild radius R_S (instead of R_S and R_{0a} at the same time). Therefore, R_S could be used as a scale of cosmological distances.

Fig. 2 shows the redshift distance Eq. (32) normalized to the distance R_{0a} for various values of the parameter B_0.

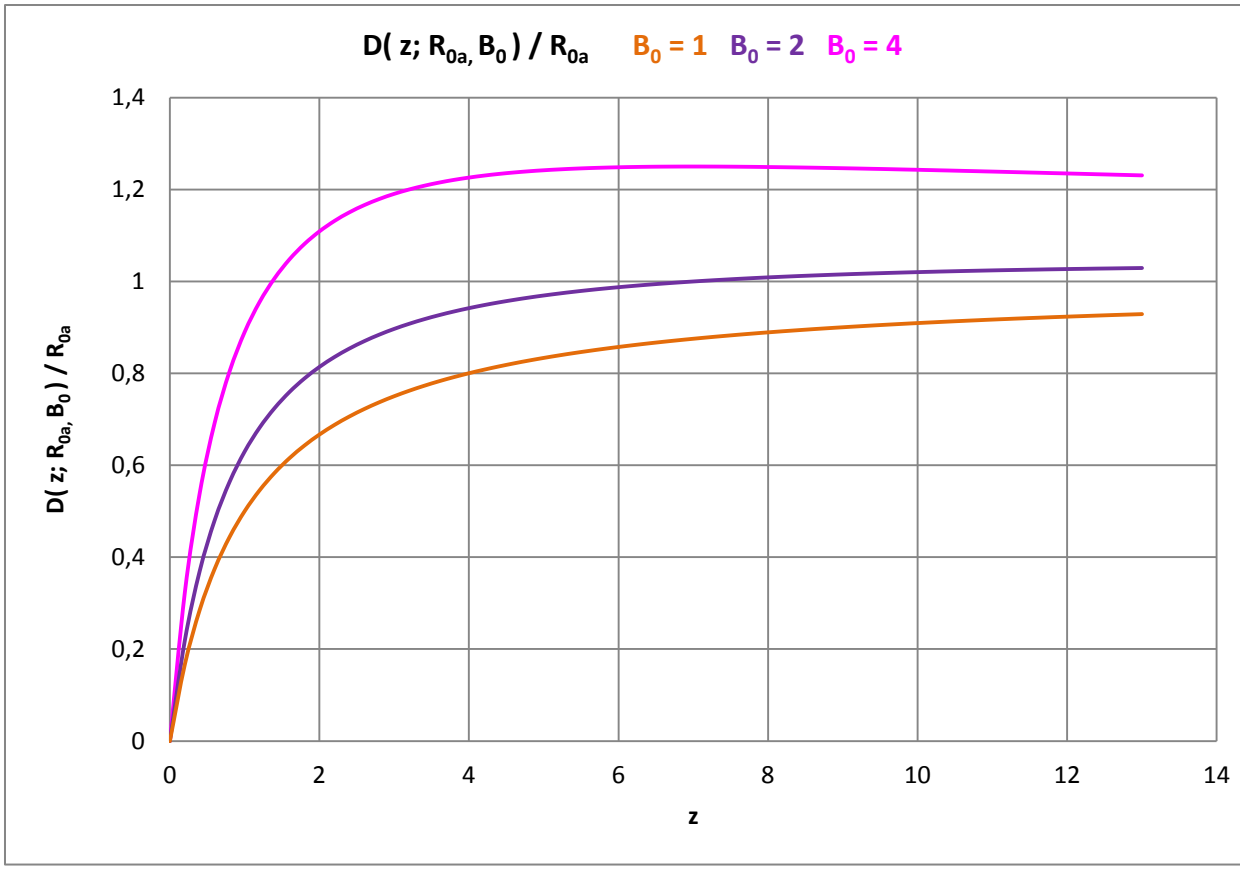

Figure 2. Redshift distance for different values of the parameter B_0.

The curvature of all the curves is a direct consequence of the Friedmann equation.

The comparison of Eq. (32) and Eq. (35), respectively, with a Hubble diagram thus determines the current radius $R_{0a} = a_0 r_a$ of the Friedmann sphere (today's physical location of the observer) and its Schwarzschild radius R_S.

Overall, each observer is located on the surface of all imaginable Friedmann spheres around him. This means that for each viewing direction a Friedmann sphere with the radius R_{0a} belongs. The extra-galactic objects (placed on $r = r_e$) observed by him then all lie according to their redshift z on a radial line somewhere between the observer (placed on $r = r_a$) and normally the center of the Friedmann sphere (placed on r = 0).
If $B_0 > 1$ it can be that $D(z) > R_{0a}$ is valid. In this case, the co-moving coordinate r_e is negative. This means, that the observer can see cosmic objects beyond the origin of coordinates (r = 0). The reason for this is the bigger velocity of light in the past in comparison with today.

Outside of every imaginable Friedmann sphere around the observer - means here the opposite of observer - there is also mass, which, however, has no gravitational effect to the place of the observer.

It should be mentioned extra that the conceivable Friedmann spheres naturally at least partially overlap.

An increasing distance $R_a(t)$ decreases with time the velocity V(t) introduced with Eq. (36), because R_S is a constant.

Because Eq. (32) and Eq. (35), respectively, describes the physical behavior of photons in the universe, the velocity V_0 in Eq. (36c) could be interpreted as an "effective" speed of light c_{0*} in vacuum:

$$V_0 = \frac{1}{2}\sqrt{\frac{2GM_{Fs}}{R_{0a}}} = \frac{c_0}{2}\sqrt{\frac{R_S}{R_{0a}}} \equiv c_{0*} \quad . \tag{36d}$$

This velocity changes actually according to $R_a(t)$ and $\rho(t)$, respectively, over the time and would have for us as today's observers just the value of the vacuum velocity c_0 that we can measure today if $B_0 = 1$ would be true. However, the analysis of measurement data will show that $B_0 > 1$ is valid.

If this interpretation is correct, the effective speed of light c_{0*} was infinitely large at the beginning of the expansion of the universe, because at that time the Friedmann sphere was infinitely small and its matter density was infinitely large, respectively. There is therefore no problem with speeds, which are apparently greater than today's speed of light, when looking into the visible universe.

2.4 Hubble parameter

For calculating the Hubble parameter we make a Taylor series expansion of our redshift distance (32) up to first order in z and find

$$D(z; R_{0a}, \mathrm{B}_0) \approx \frac{1}{3} R_{0a}(\mathrm{B}_0 + 2)z + ... \quad . \tag{37}$$

This results in

$$c_0 z \approx \frac{3c_0}{R_{0a}(B_0 + 2)} D \quad . \tag{38}$$

This is how we find the today's Hubble parameter

$$H_{0a}(R_{0a}, B_0) \approx \frac{3c_0}{R_{0a}(B_0 + 2)} \quad . \tag{39}$$

Our today's Hubble parameter H_{0a} depends on the two parameters R_{0a} and B_0 and is in this form valid only for small redshifts because of the series expansion made. This means that this H_{0a} is only valid locally near the observer.

The reciprocal of the Hubble parameter is the Hubble time t_{H0a} and yields

$$\frac{1}{H_{0a}} = t_{H_{0a}} \approx \frac{(B_0 + 2)}{3}\frac{R_{0a}}{c_0} \quad . \tag{40}$$

This Hubble time is not the same how Eq. (11).

If we consider the today's Hubble parameter Eq. (39) for small redshifts as a definition, we can write the redshift distance via

$$B_0 \approx \frac{3c_0}{H_{0a}R_{0a}} - 2 \quad . \tag{39a}$$

also like this

$$D(z; R_{0a}, B_0) \approx \frac{R_{0a}}{(z+1)^{\frac{2}{3}}}\left\{\left(3\frac{R_{H0a}}{R_{0a}} - 2\right)\left[1 - \frac{1}{(z+1)^{\frac{1}{3}}}\right] + (z+1)^{\frac{2}{3}} - 1\right\} \quad . \tag{41}$$

The quotient $R_{H0a} = c_0/H_{0a}$ is called the Hubble radius in the astrophysical literature. For this distance, the escape speed by definition reaches the speed of light if it is assumed that a linear Hubble law is valid for all distances, which is - of course - a very rough approximation.
The Eq. (41) is only valid for small redshifts how the Eqs. (37) and (39) itself.

2.5 The magnitude-redshift relation

The magnitude-redshift relation results by the general definition of the apparent magnitude m

$$m - m_{0a} = 5\log_{10}\frac{D}{R_{0a}} \quad . \tag{42}$$

Here an apparent limit magnitude m_{0a} was introduced instead of R_{0a}, which also changes with time. Substituting Eq. (32) into Eq. (41) then provides the sought magnitude-redshift relation

$$m(z; m_{0a}, B_0) = 5\log_{10}\left\{B_0\left[1 - \frac{1}{(z+1)^{\frac{1}{3}}}\right] + (z+1)^{\frac{2}{3}} - 1\right\} - \frac{10}{3}\log_{10}(z+1) + m_{0a} \quad . \tag{43}$$

The two free parameters m_{0a} and B_0 can be determined by direct comparison with a suitable magnitude-redshift diagram of astrophysical objects.

2.6 The angular size-redshift relation

This relation results in for larger distances over

$$\varphi = \arcsin\frac{\delta}{D} \approx \frac{\delta}{D} \tag{44}$$

to

$$\varphi(z;\delta/R_{0a},B_0) \approx \frac{\delta}{R_{0a}} \frac{(z+1)^{\frac{2}{3}}}{\left\{B_0\left[1-\frac{1}{(z+1)^{\frac{1}{3}}}\right]+(z+1)^{\frac{2}{3}}-1\right\}} \quad . \tag{45}$$

In this equation φ means the measurable angular size and δ the linear size of the observed extra-galactic object.

2.7 The number-redshift relation

In flat Euclidean space the equation for the light-path sphere becomes to

$$V = \frac{4\pi}{3} D^3 \quad . \tag{46}$$

If we introduce the redshift distance via Eq. (32)

$$V(z;R_{0a},B_0) = \frac{4\pi}{3} \frac{{R_{0a}}^3}{(z+1)^2} \left\{B_0\left[1-\frac{1}{(z+1)^{\frac{1}{3}}}\right]+(z+1)^{\frac{2}{3}}-1\right\}^3 \tag{47}$$

we get for the number-redshift relation

$$N(z;R_{0a},B_0) = \frac{N_{0a}}{(z+1)^2} \left\{B_0\left[1-\frac{1}{(z+1)^{\frac{1}{3}}}\right]+(z+1)^{\frac{2}{3}}-1\right\}^3 \quad , \tag{48}$$

where N_{0a} means the expected number of objects in the whole light-path sphere V_{0a} and besides

$$N_{0a} = V_{0a}\eta = \frac{4\pi}{3} R_{0a}{}^{3}\eta \qquad and \qquad N = V\eta \tag{49a, b}$$

applies. With η the number density was named.

In logarithmic form results

$$\log_{10} V(z; R_{0a}, B_0) = 3\log_{10}\left\{ B_0\left[1 - \frac{1}{(z+1)^{\frac{1}{3}}}\right] + (z+1)^{\frac{2}{3}} - 1\right\} - 2\log_{10}(z+1) + \log_{10} N_{0a} \quad . \tag{50}$$

3. Derivation of further physical redshift distances

The starting point for the derivation of the further redshift distances are the following elementary equations

$$(z+1)^{\frac{2}{3}} = \frac{a_0}{a_e} \qquad Eq.(25) \qquad and \qquad D = R_{0a} - R_{ee} \qquad Eq.(19)$$

and

$$(z+1)^{\frac{2}{3}} = \frac{a_0 r_a}{a_e r_a} = \frac{R_{0a}}{R_{ea}} \qquad and \qquad (z+1)^{\frac{2}{3}} = \frac{a_0 r_e}{a_e r_e} = \frac{R_{0e}}{R_{ee}} \tag{51}$$

and

$$D_e = R_{ea} - R_{ee} = \frac{R_{0a}}{(1+z)^{\frac{2}{3}}} - (R_{0a} - D) = R_{0a}\left[\frac{1}{(1+z)^{\frac{2}{3}}} - 1\right] + D$$

because of

$$R_{ee} = R_{0a} - D \qquad and \qquad R_{ea} = \frac{R_{0a}}{(1+z)^{\frac{2}{3}}} \tag{52}$$

and also

$$D_0 = R_{0a} - R_{0e} = R_{0a} - (1+z)^{\frac{2}{3}}(R_{0a} - D)$$

because of

$$R_{0e} = (1+z)^{\frac{2}{3}}(R_{0a} - D) \quad . \tag{53}$$

This results in the following further distances

$$R_{ee} = R_{0a} - D \qquad and \qquad R_{ea} = \frac{R_{0a}}{(1+z)^{\frac{2}{3}}}$$
$$and \qquad R_{0e} = (1+z)^{\frac{2}{3}} R_{ee} = (1+z)^{\frac{2}{3}} (R_{0a} - D) \quad . \tag{54}$$

R_{ee} is the distance at that time between the galaxy observed emitting the light and the origin of the coordinates at the time t_e the light was emitted (t_e: time at that time).

R_{ea} is the distance at that time of the observer's galaxy from the origin of the coordinates.

R_{0e} is the today's - at time t_0, at which the light is absorbed on the place of observer - distance of the light-emitting galaxy from the origin of the coordinates.

R_{0a} is today's distance of the galaxy containing the observer from the origin of the coordinates.

These distances become concretely with Eq. (32)

$$R_{ee}(z; R_{0a}, B_0) = R_{0a}\left\{1 - \frac{1}{(z+1)^{\frac{2}{3}}}\left\{B_0\left[1 - \frac{1}{(z+1)^{\frac{1}{3}}}\right] + (z+1)^{\frac{2}{3}} - 1\right\}\right\} \tag{55}$$

and

$$R_{0e}(z; R_{0a}, B_0) = R_{0a}\left\{1 - B_0\left[1 - \frac{1}{(z+1)^{\frac{1}{3}}}\right]\right\} \tag{56}$$

and of course too

$$R_{ea}(z; R_{0a}) = \frac{R_{0a}}{(1+z)^{\frac{2}{3}}} \quad . \tag{57}$$

These distances from the origin of coordinates yield

$$D_e(z; R_{0a}, B_0) = R_{0a}\frac{B_0}{(z+1)^{\frac{2}{3}}}\left[1 - \frac{1}{(z+1)^{\frac{1}{3}}}\right] \quad . \tag{58}$$

D_e is the distance at that time t_e between the observed galaxy and the galaxy in which the observer is located.

Furthermore we find

$$D_0(z; R_{0a}, B_0) = R_{0a} B_0 \left[1 - \frac{1}{(z+1)^{\frac{1}{3}}} \right] \quad . \tag{59}$$

D_0 is the today's distance between the two participating galaxies.

The following figures illustrate the equations for the further redshift distances, where we have normalized all distances to R_{0a}.

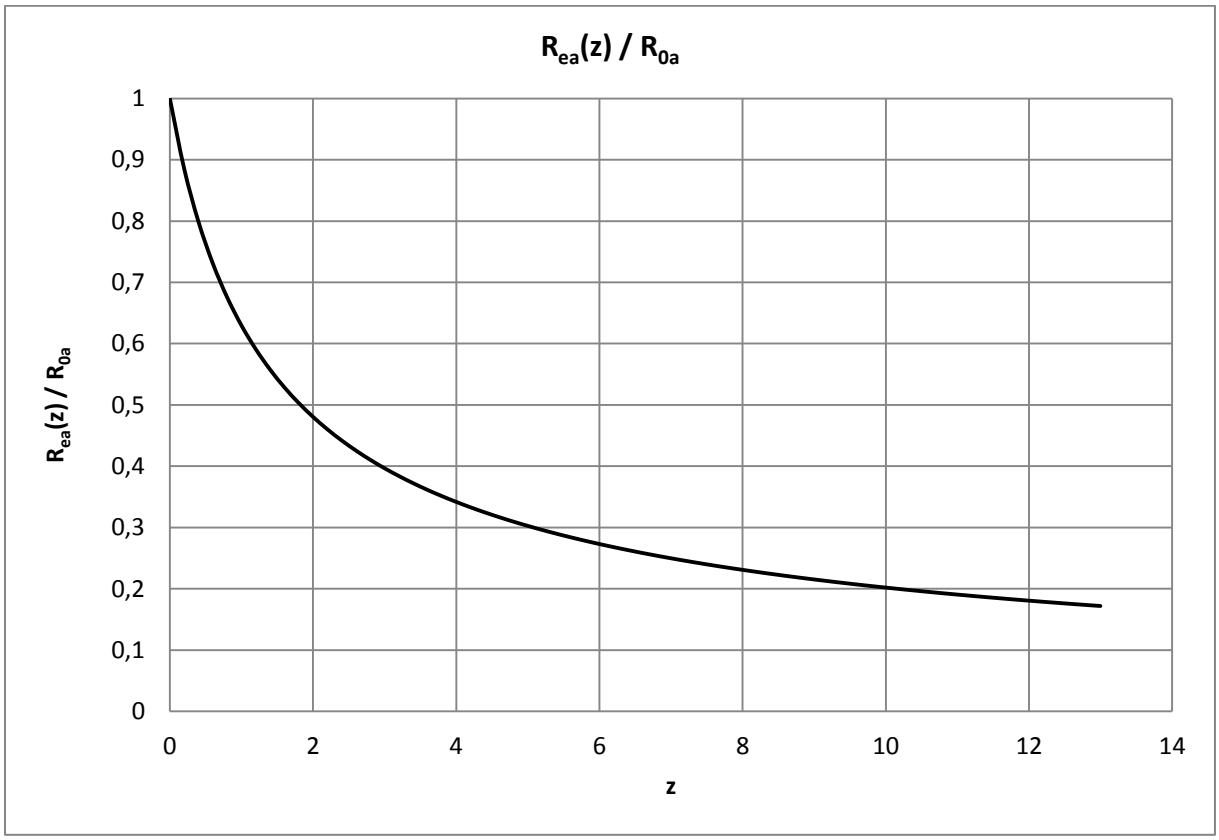

Figure 3. Redshift distance R_{ea} normalized to the distance R_{0a}.

This distance is not depending on parameter $B_{0.}$

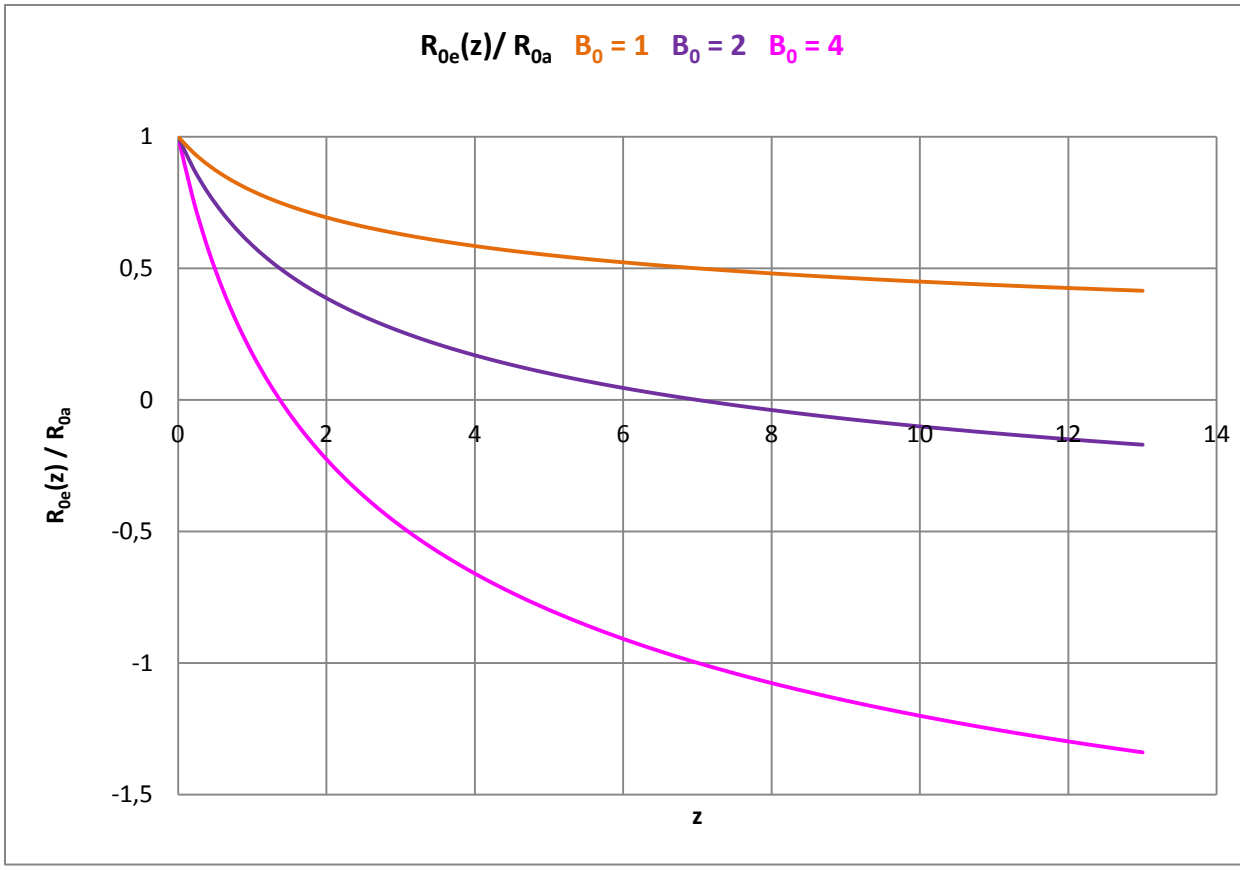

Figure 4. Redshift distance R_{0e} normalized to the distance R_{0a} for various values of the parameter B_0.

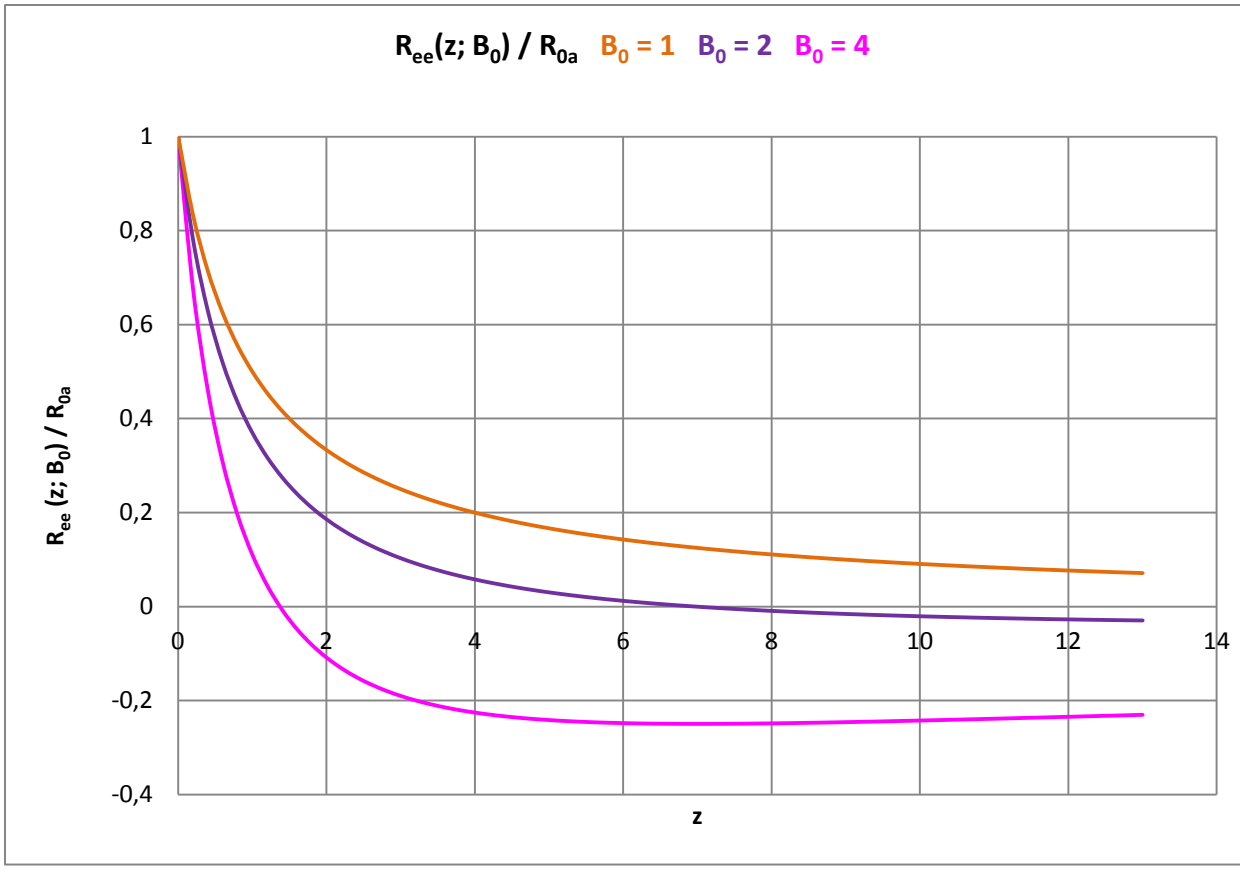

Figure 5. Redshift distance R_{ee} normalized to the distance R_{0a} for different values of the parameter B_0.

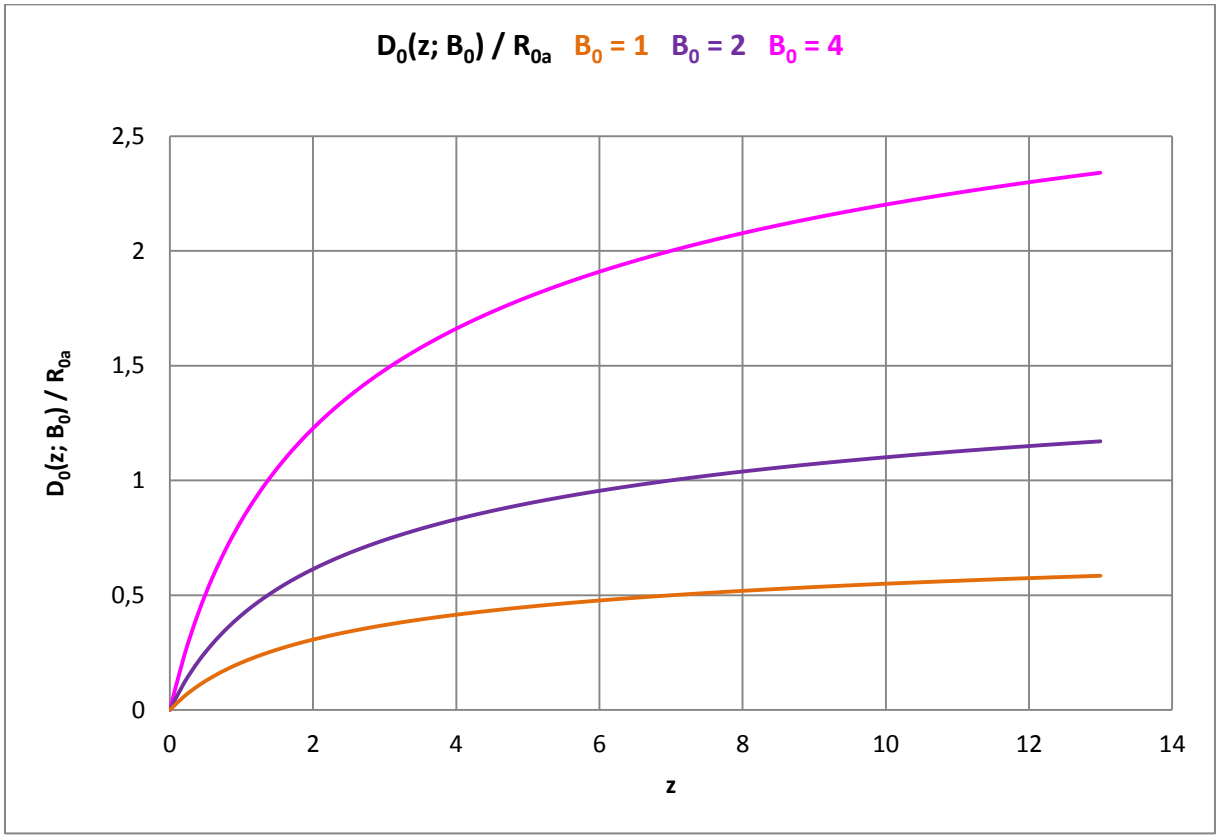

Figure 6. Today's redshift distance D_0 normalized to the distance R_{0a} for various values of the parameter B_0.

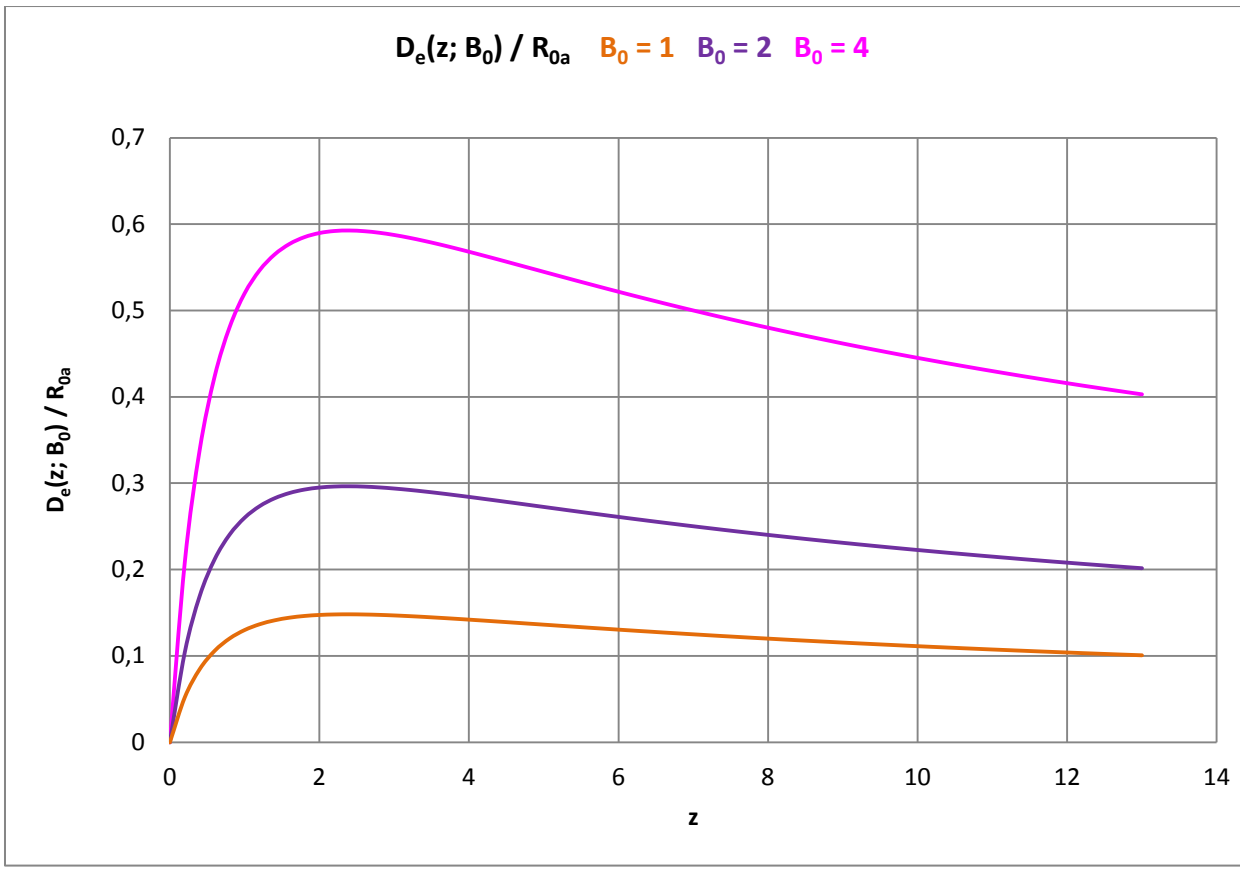

Figure 7. The redshift distance at that time D_e normalized to the distance R_{0a} for various values of the parameter B_0.

An observed cosmic object lies behind the origin of coordinates if the distance - R_{ee} and R_{0e}, respectively - to this has a negative value because of $r_e < 0$.

In the specialist literature, none of these redshift distances are known and they cannot be derived there, respectively.

We will give concrete values for such redshift distances for the galaxy M87 and 27 SN Ia below.

4. Determination of the parameter values

The present paper presents a theoretical derivation of some redshift distances, which we carry out without approximations for e.g. small redshifts z and is mainly of theoretical nature. The essay is therefore a theoretical offer to the observing cosmologists.

Nevertheless, in this chapter we will apply the theory presented here in detail to some measurement results of observational cosmology, whereby we only demonstrate the principle of evaluating the measurement data. For this reason, no more detailed error analyzes are carried out. We leave that to the interested experts of observational cosmology.

4.1 Magnitude-redshift relation

The apparent magnitude m depends according to Eq. (43) in addition to the measurable redshift z also on the two parameters B_0 and m_{0a}.

To find the values of the parameters, the quasar catalog by Véron-Cetty et al. [1] is suitable in which measured redshifts and apparent magnitudes of 132,975 quasars are given.

Fig. 8 shows all these quasars in a single magnitude-redshift diagram, where we have used $\log_{10}(cz)$ on the axis of ordinates.

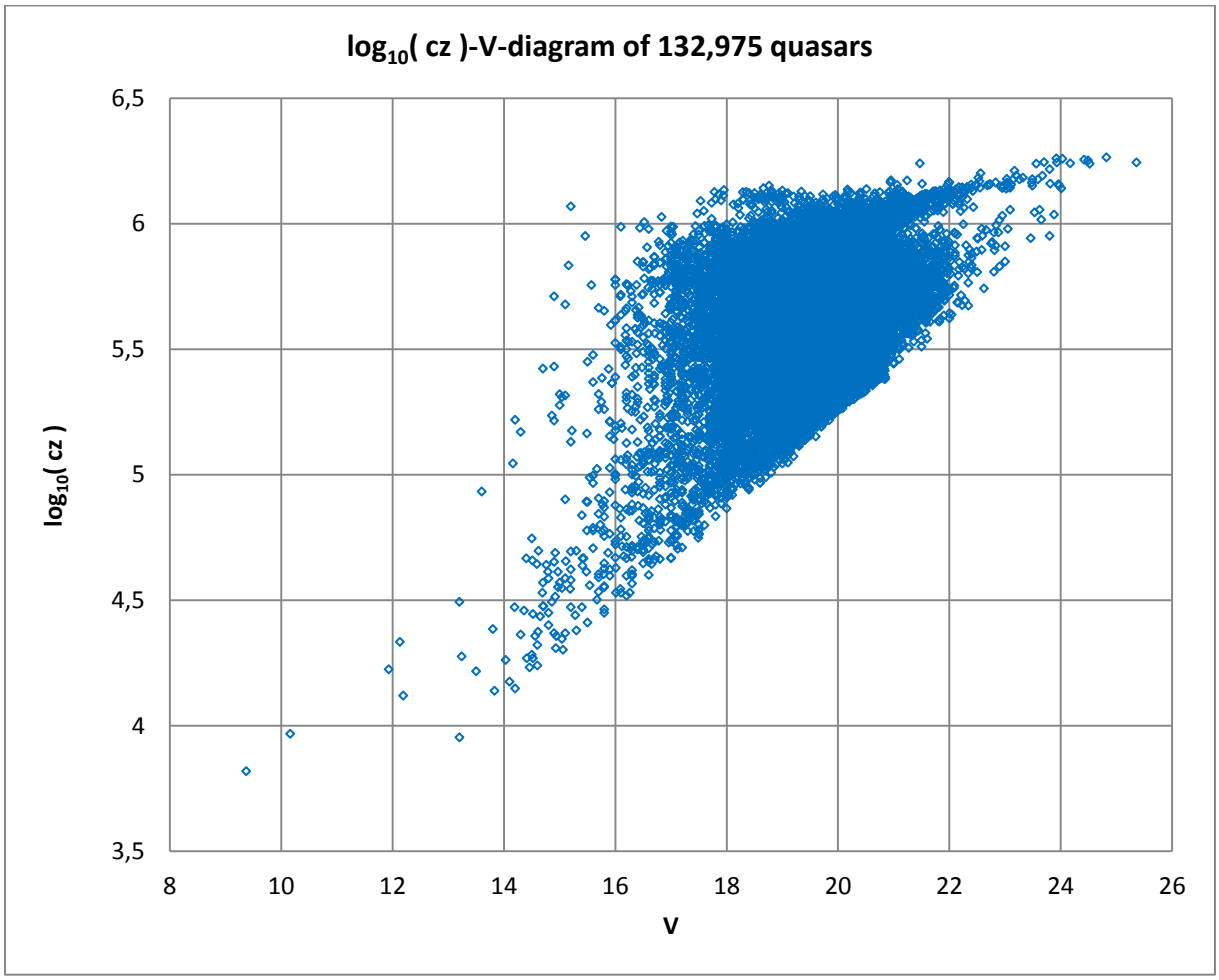

Figure 8. Magnitude-redshift diagram for all 132,975 quasars according to M.-P. Véron-Cetty et al. [1].

A clear edge exists on the right side of the accumulation of measurement points, which indicates minimum apparent magnitudes for associated redshifts. The apparent magnitudes are usually up to far to the left of this edge inside the diagram.

If we form redshift intervals with mean values of the redshifts and the corresponding mean values for the apparent magnitude, this fact leads to a clear curvature of the mean value curve in the direction of the redshift axis. This curvature should be explained by means of a valid astrophysical theory. More precisely: The theory has to explain the curvature! This suggests that our redshift distance [i.e. ultimately Eq. (32)] could be suitable for the measured values.

It is precisely such a strange magnitude-redshift diagram, which was stimulating us to think about cosmological distance determinations for many years [9].

To evaluate the quasar data set, we first create 75 z-intervals with 1,773 quasars each. For these intervals, we calculate the mean values $<z_i>$ and the associated mean values $<m_i>$ of the quasars.

We use the following χ^2-function

$$\chi^2(p_k) = \frac{1}{(N-1)} \sum_{i=1}^{N} \left[m_{th,i}(p_k) - m_{obs,i} \right]^2 \tag{60}$$

for our evaluation of the data.
The abbreviation p_k with k = 1 and 2 stands for the two parameters we are looking for, B_0 and m_{0a}.

If we use our magnitude-redshift relation Eq. (43), the χ^2-function looks more concrete

$$\chi^2(z_i, B_0, m_{0a}) = \\ = \frac{1}{(N-1)} \sum_{i=1}^{N} \left[5 \log_{10} \left\{ B_0 \left[1 - \frac{1}{(z_i+1)^{\frac{1}{3}}} \right] + (z_i+1)^{\frac{2}{3}} - 1 \right\} - \frac{10}{3} \log_{10}(z_i+1) + m_{0a} - m_{obs,i} \right]^2 . \tag{60a}$$

Using the quasar data and the usual mathematical procedure, we find the parameters to be $B_0 = 3.237$ and $m_{0a} = 19.836$.

Fig. 9 shows the result of the mean value formation and the adaptation of our theory to the curvature of the mean value curve.

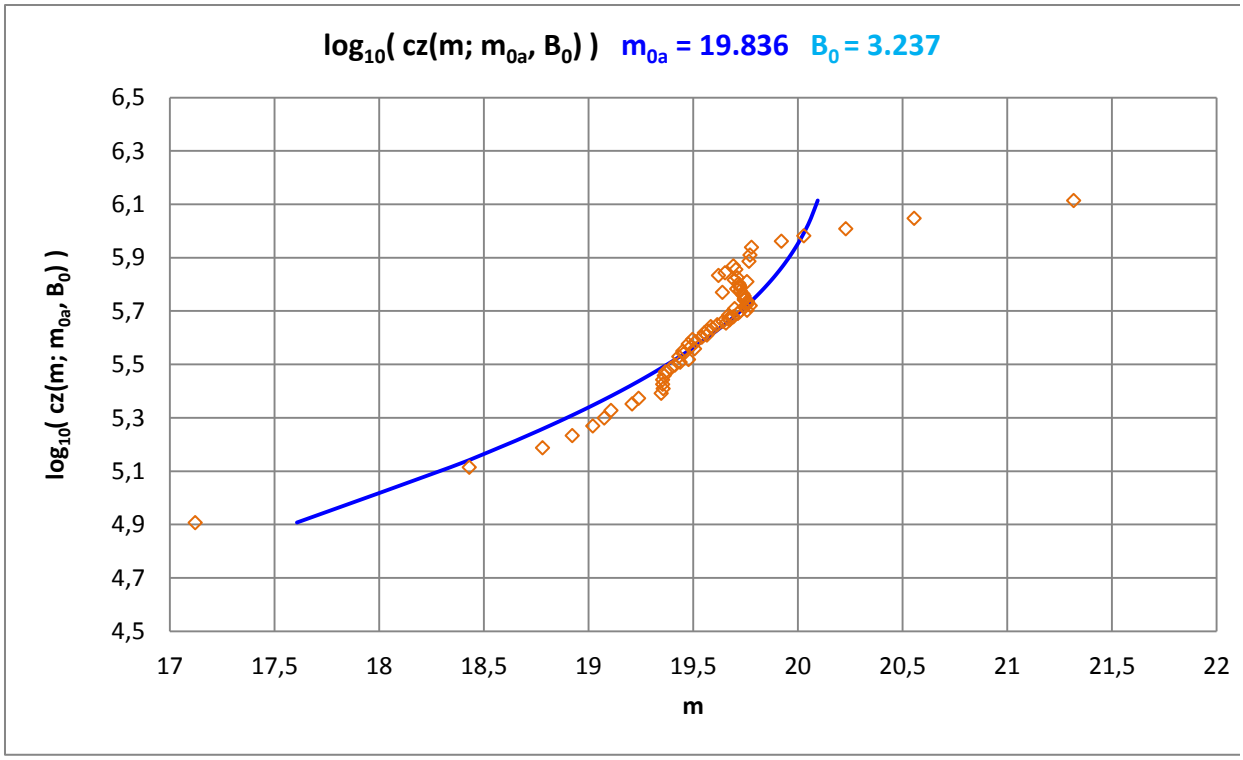

Figure 9. Magnitude-redshift diagram for 132,975 quasars according to M.-P. Véron-Cetty et al. [1].

From our point of view, a possible interpretation of the measured magnitude-redshift relation may be:
The quasars came in to being historically slowly as relatively few and weakly luminous objects at a point in time that corresponds to about $z \approx 4.3$ (development effect). The quasars later behaved as our theory expects in modified flat space and moved with time - i.e. for decreasing redshifts z - on average along the theoretical curve (in the diagram from top right diagonally to bottom left). Then the quasars have gradually died out in the recent past and became relatively bright in this process.

4.2 Number-redshift relation

We use the following variance to evaluate the number-redshift relation

$$\chi^2(p_k) = \frac{1}{(N-1)} \sum_{i=1}^{N} \left[N_{th,i}(p_k) - N_{obs,i} \right]^2 \quad . \tag{61}$$

The abbreviation p_k with k = 1 and 2 stands for the two parameters we are looking for, B_0 and N_{0a}.

If we insert our number-redshift relation Eq. (48), the Eq. (61) reads concrete

$$\chi^2(z_i, B_0, N_{0a}) =$$

$$= \frac{1}{(N-1)} \sum_{i=1}^{N} \left[3\log_{10} \left\{ B_0 \left[1 - \frac{1}{(z_i+1)^{\frac{1}{3}}} \right] + (z_i+1)^{\frac{2}{3}} - 1 \right\} - 2\log_{10}(z_i+1) + \log_{10} N_{0a} - N_{obs,i} \right]^2 \quad . \tag{61a}$$

Using simple mathematics, we find N_{0a} = 85,692 for the theoretically expected total number of quasars and B_0 = 3.427 results.

The expected number N_{0a} is some smaller than the number of quasars given within the catalogue of M.-P. Véron-Cetty et al. [1]. This indicates a certain incompleteness of the measurements, because N_{0m} means the sum of all objects which should be found up to z = ∞ (see chapter 2.7). May be that development effects have to be involved also, but such effects are not the object of our theoretical contemplations.

May be that more measurement values would get a better agreement between theory and reality.
May be that the astronomers have measured to few quasars having big redshifts until now.
May be that the some smaller number theoretical expected means that the theory using the mFLRWM describes the cosmological reality - the number of cosmic object in this case - not in a right way.

Fig. 10 shows the graphic result.

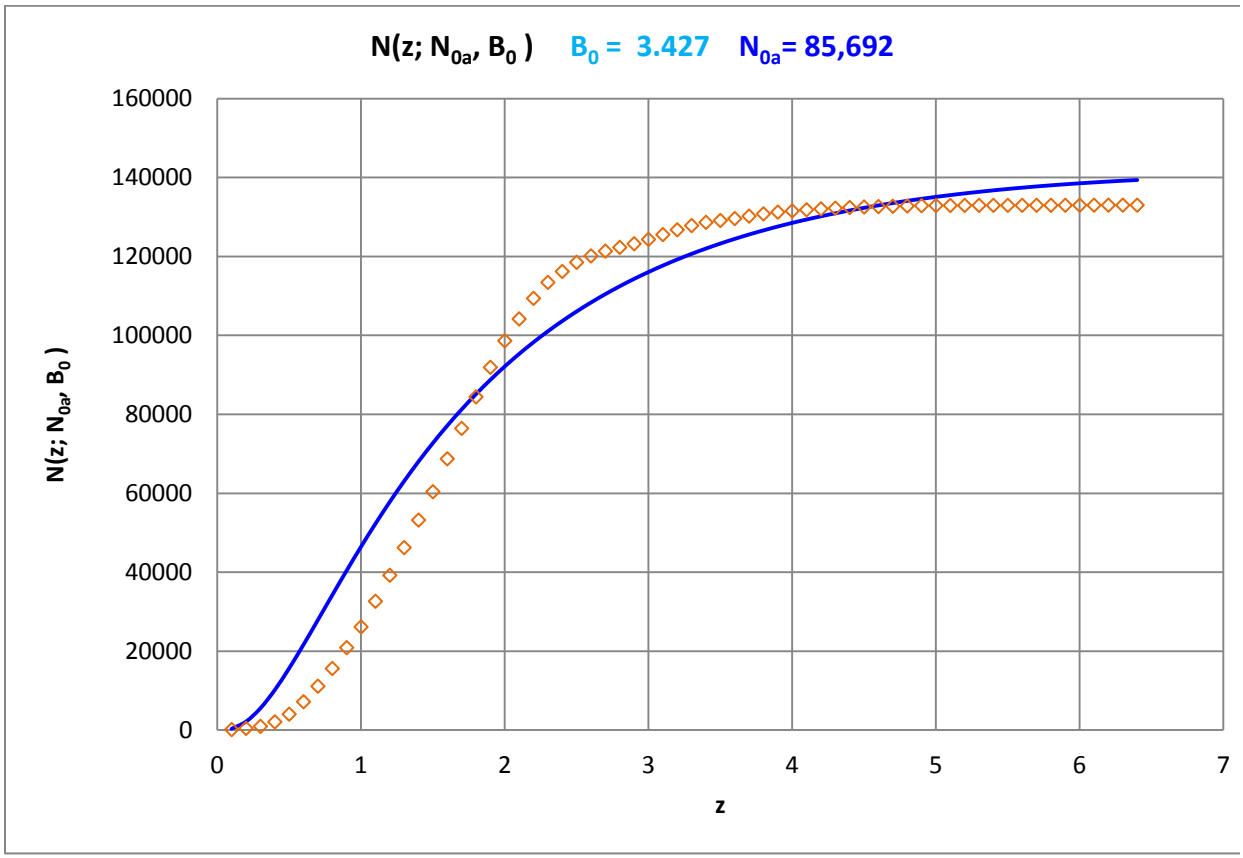

Figure 10. Number-redshift diagram for the 132,975 quasars according to M.-P. Véron-Cetty et al. [1].

4.3 Angular size-redshift relation

In this case, we use the measurement data from K. Nilsson et al. [2] to find an average linear size of the cosmic objects measured there.

The starting point is the variance

$$\chi_{\varphi}^{\,2}(p_k) = \frac{1}{(N-1)} \sum_{i=1}^{N} \left[\varphi_{th,i}(p_k) - \varphi_{obs,i} \right]^2 \quad . \tag{62}$$

The abbreviation p_k with k = 1and 2 stands for the two parameters we are looking for, B_0 and δ/R_{0a}.

If we use our angular size-redshift relation Eq. (45), the Eq. (61) reads concrete

$$\chi_{\varphi}^{\,2}\left(z_i, \frac{\delta}{R_{0a}}, B_0 \right) = \frac{1}{(N-1)} \sum_{i=1}^{N} \left[\frac{\delta}{R_{0a}} \frac{(z_i+1)^{\frac{2}{3}}}{\left\{ B_0 \left[1 - \frac{1}{(z_i+1)^{\frac{1}{3}}} \right] + (z_i+1)^{\frac{2}{3}} - 1 \right\}} - \varphi_{obs,i} \right]^2 \quad . \tag{62a}$$

The comparison of the theory with the measurement data using $\langle B_0 \rangle = 3.334$ results in a value of $\delta/R_{0a} = 6.7799 \times 10^{-5}$. $\langle B_0 \rangle$ means the mean value of both parameters B_0 found: Analyzing m(z)- and N(z)-relation, respectively.

Fig. 11 shows the graphic result.

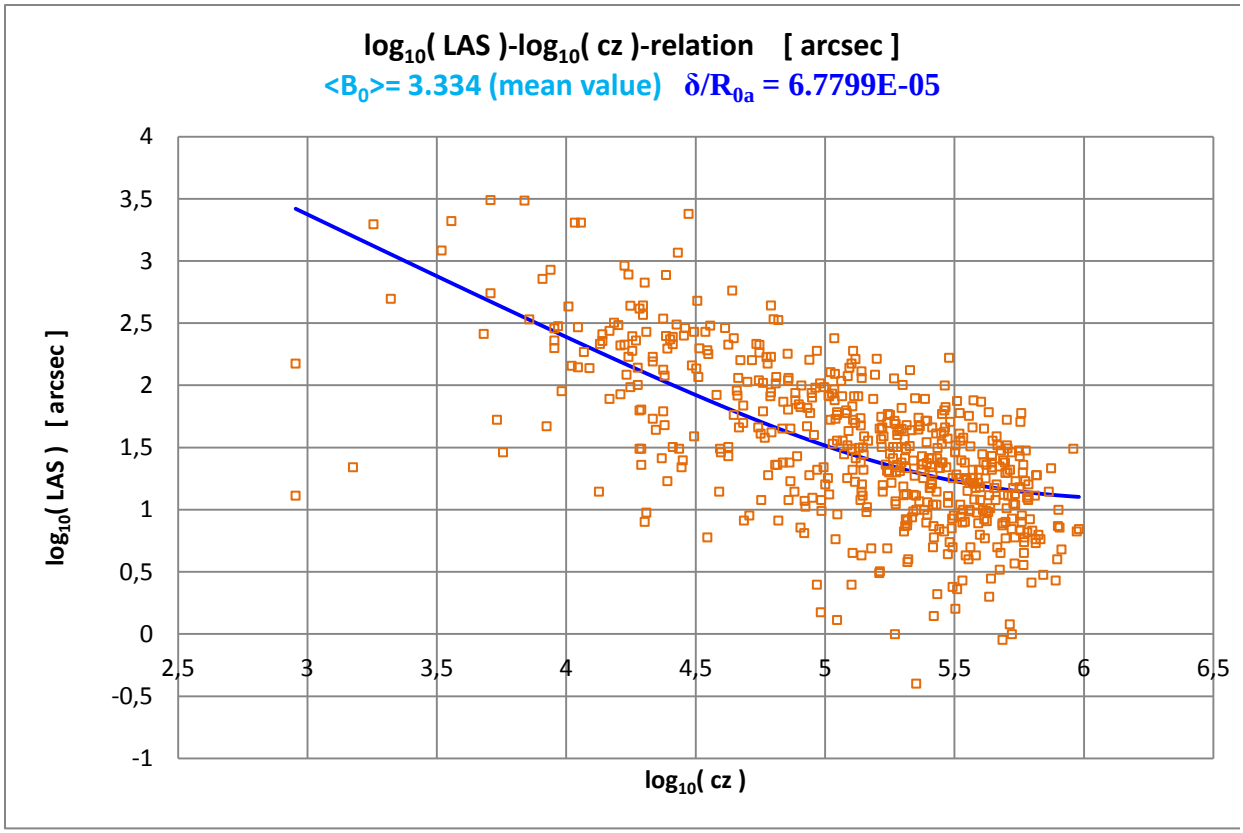

Figure 11. Angular size-redshift diagram according to K. Nilsson et al. [2].

The determination of the linear size δ requires the knowledge of R_{0a}. Because the absolute magnitudes are known for some SN Ia (which differ strangely enough slightly from one another), we can determine R_{0a} using a magnitude-redshift diagram of these cosmic objects. We will carry out this within the next chapter.

4.4 Fixing of R_{0a} with the help of SN Ia

By W. L. Freedman et al. [3], data from a total set of 27 SN Ia were made available, with the help of which we can determine both the distance R_{0a} - the observers current physical distance from an origin of coordinates - and, as a main result, the today's Hubble parameter H_{0a}.

The data we are interested in are the distance modules (μ_{TRGB} and μ_{Ceph}, respectively), the maximum apparent magnitudes (m_{CSP_B0} and m_{SC_B}, respectively) and the radial velocities V_{NED}, from which the redshifts z_{NED} can be calculated.

The methods taken into account in [3] for determining the maximum apparent magnitude and thus the associated absolute magnitude are different, which is why somewhat different values are given for one and the same SN Ia. For our purposes, we calculate the mean values from these data and assign them to the relevant SN Ia.

We calculate the absolute magnitudes M_i of the SN Ia_i using (μ_{TRGB} - m_{CSP_B0}) and (μ_{Ceph} - m_{SC_B}), respectively, and then we always calculate an average value $<M_i>$ if both value pairs are specified for one and the same SN Ia. From all the absolute magnitudes obtained in this way, we finally form the mean value of the absolute magnitude to be $<M> \approx -19.245$, which enables us to determine the distance R_{0a} with the aid of the parameter m_{0a}, which results from the magnitude-redshift diagram of the SN Ia. The simple equation used for this is

$$R_{0a} = 10^{\frac{(m_{0a} - <M>)}{5} + 1} \quad . \tag{63}$$

The graphic result is shown in Fig. 12.

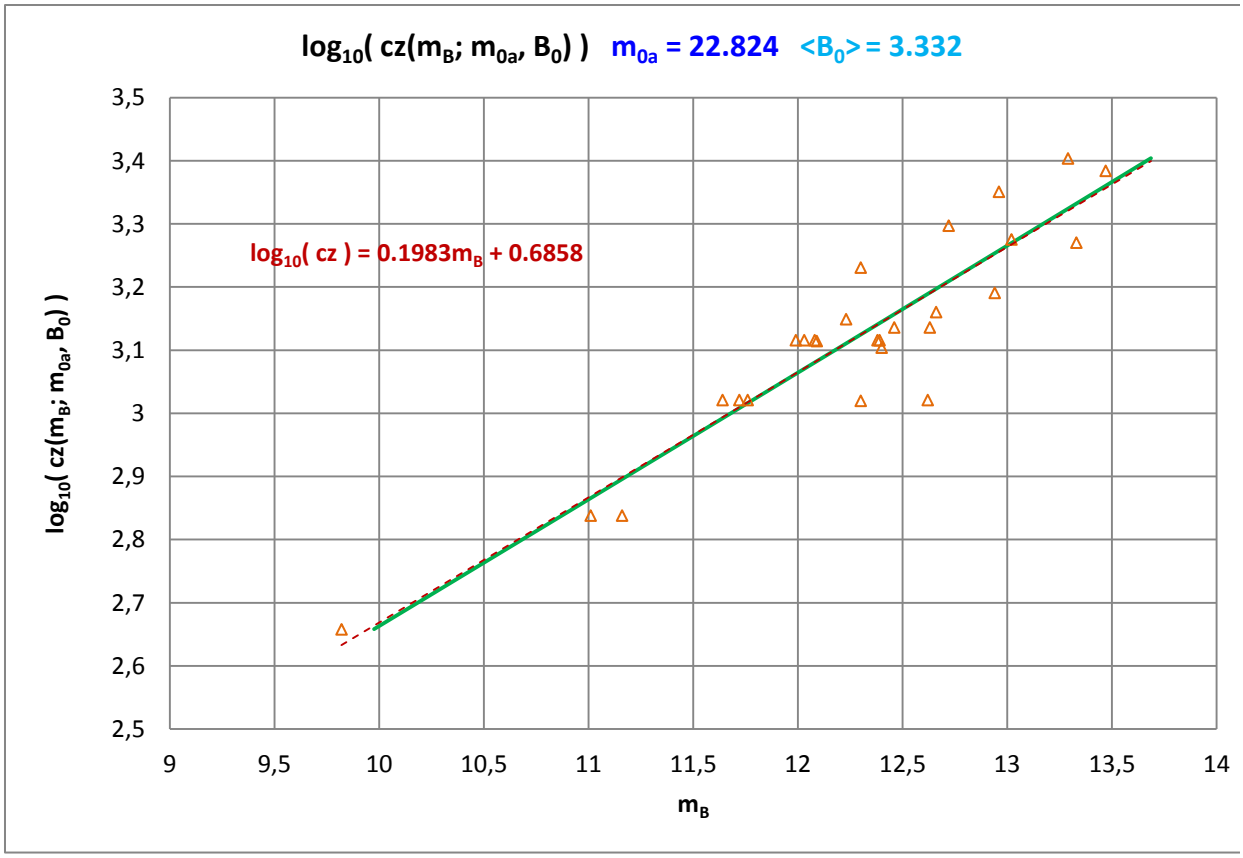

Figure 12. Magnitude-redshift diagram for 27 SN Ia according to W. L. Freedman et al. [3].

The theoretical curve (green) lies nearly exact on the linear trend line (dashed in red), the equation of which is given in the figure.

Finding $m_{0a} \approx 22.824$ and using the mean value of the absolute brightness $<M> = -19.245$, the distance $R_{0a} \approx$ 2,586.938 Mpc we are ultimately looking for is the essential result of this data analysis.

With the help of the value of R_{0a} and taking the Eq. (39), which is an approximation for small redshifts, the today's Hubble parameter $H_{0a} \approx 65.2$ km/(s·Mpc) results. This value is slightly below the Planck value (2018) with $H_{0,Planck} \approx 67.66$ km/(s·Mpc) [4].

In Table 9 in the appendix, all the values we have used for the magnitude-redshift diagram of the 27 SN Ia are compiled.

Using Eq. (33a) and Eq. (A20) for today, we get as result for the today's mass density

$$\rho_0 = \frac{3}{2\pi G} \frac{{c_0}^2}{{R_{0a}}^2 {B_0}^2} \quad . \tag{64}$$

With the help of parameters, $<B_0>$ and R_{0a} determined by us, we find $\rho_0 \approx 9.088 \times 10^{-30}$ g/cm^3 for today's matter density inside the Friedman sphere.

Via

$$M_{Fs} = \frac{4\pi}{3} {R_{0a}}^3 \rho_0 = 2 \frac{{c_0}^2 R_{0a}}{G {B_0}^2} \tag{65}$$

the constant mass of the Friedmann sphere results in $M_{Fs} \approx 1.94 \times 10^{55}$ g.

Because we generally do not consider the accuracy within this paper, we simply specify the decimal places with up to three places, whereby the mathematical analysis of the data usually delivers more decimal digits.

Using Eq. (33c) we find for the Schwarzschild radius $R_S \approx 931.949$ Mpc.

With the known value $R_{0a} \approx 2{,}586.938$ Mpc we can calculate the mean linear size of the Nilsson objects [2] to be $\delta \approx 0.175$ Mpc, because we have found $\delta/R_{0a} = 6.7799 \times 10^{-5}$ for them.
Using known R_{0a} and $<B_0>$, of course, all linear dimensions of these objects can be calculated using their angular size and redshift if they could be measured.

4.5 Calculation of all possible redshift distances for the SN Ia

4.5.1 Absolute values of redshift distances

Because we were able to determine R_{0a}, we can graphically display all theoretical possible redshift distances in a form, which is not normalized to R_{0a}. Fig. 13 shows the result, using the values we found for $<B_0>$ and R_{0a}.

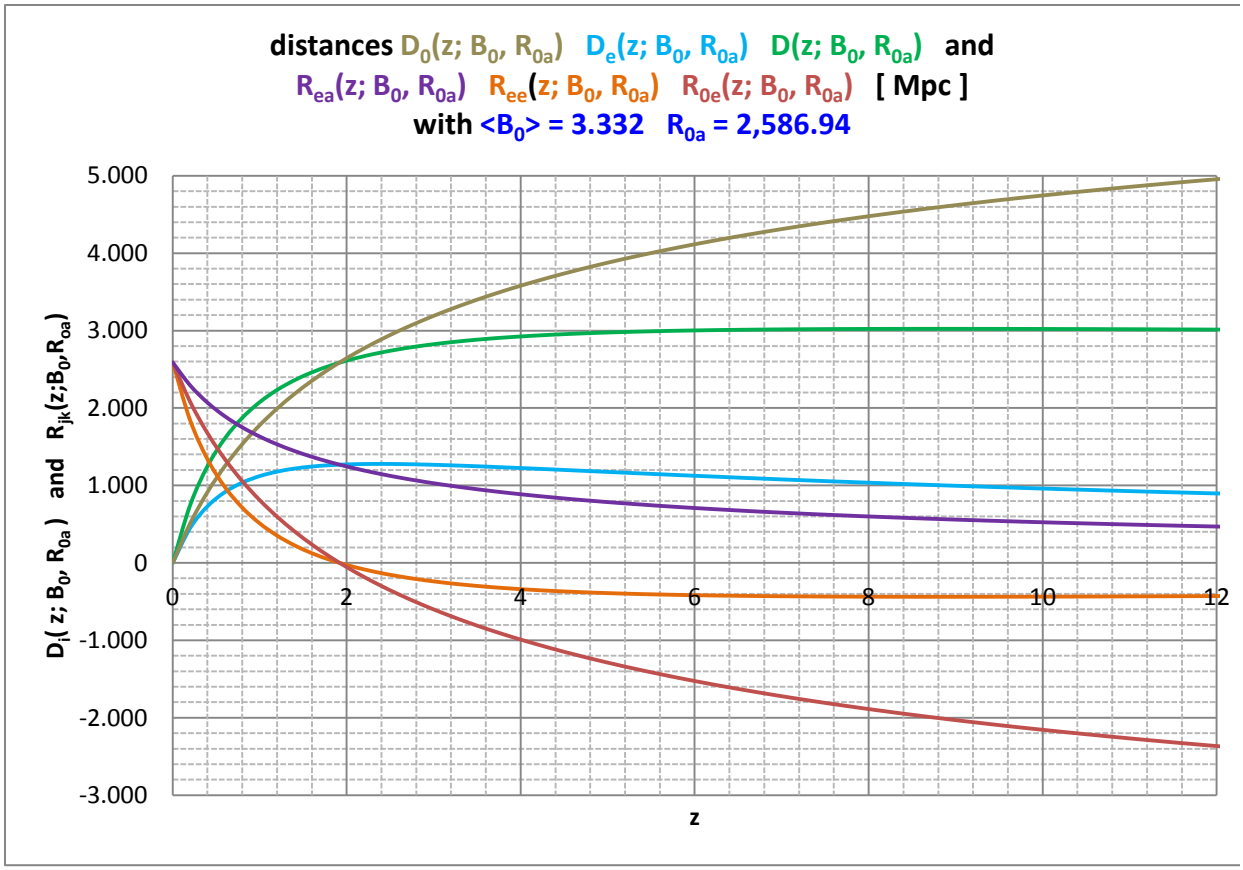

Figure 13. Redshift distance D (real light path) and all further possible redshift distances D_i (i = 0, e) and R_{jk} (j = 0, e; k = e, a) as a function of the redshift up to z = 12.

To interpret Fig. 13:

a) For redshift z going towards infinity the distance D goes to a value, which is greater than R_{0a}. This means that the observer can observe objects for which is $D > R_{0a} \approx 2{,}586.94$ Mpc if the measured redshift z is great enough; the observer can have a look on the other side of the origin of coordinates.

For z --> ∞ the redshift distance D --> ∞ results.

b) The light path distance $D = R_{0a} - R_{ee}$ is always greater than the distance D_e (time at that time) but partly smaller than the distance D_0 (today's).

In particular, the light path D is not equal to the today's distance D_0 between two astrophysical objects.

c) The distances R_{jk} are physical distances from an origin of coordinates and develop directly with the change in the scale parameter a(t) over time. For large redshifts, the scale parameter was correspondingly small and, as a result of this, the associated physical distances R_{ee} and R_{ea} were also correspondingly small.

d) Negative values of distances - e.g. R_{ee} and R_{0e} - mean that the observer can have a look as far as behind the origin of coordinates, which is mainly a fictitious one. For such distances $R_e(t) = a(t)r_e$ with $r_e < 0$ is the right equation.

e) The distance at that time D_e is interesting: It shows a maximum for a specific redshift and approaches only zero for very large redshifts.

For calculation the real redshift distances of SN Ia, we need the knowledge about possible peculiar velocities.

Therefore, we will investigate this situation for all SN Ia used in this paper within the next chapter.

4.5.2 Peculiare velocities of SN Ia

Because all SN Ia have in general the same average absolute magnitude <M> ≈ -19.245 they all have to lie on the theoretical curve in Fig. 12. As this is not the case, they must have partly peculiar velocities, which can be calculated in a simple way. The following Table 1 shows the result:

SN Ia	z_observed	z_Hubble	cz=v_not_Hubble (km/s)	SN Ia	z_observed	z_Hubble	cz=v_not_Hubble (km/s)
2011fe	0.00151772	0.00141297	31.401	2011iv	0.00435635	0.00392084	130.563
1989B	0.00229826	0.00262262	-97.241	1998aq	0.00456316	0.00478417	-66.258
1998bu	0.00229826	0.00244708	-44.615	2011by	0.00456316	0.00517607	-183.748
2001el	0.00349242	0.00444260	-284.858	2013dy	0.00470325	0.00430098	120.600
1981B	0.00350242	0.00327384	68.526	2012ht	0.00482667	0.00524851	-126.465
1990N	0.00350242	0.00515215	-494.576	1994ae	0.00517691	0.00597580	-239.501
1994D	0.00350242	0.00346059	12.540	2007sr	0.00567726	0.00444260	370.142
2012cg	0.00350242	0.00339718	31.550	2002fk	0.00621763	0.00716114	-282.856
2015F	0.00423960	0.00465309	-123.961	1995al	0.00629102	0.00620166	26.789
2012fr	0.00434300	0.00403119	93.479	2007af	0.00661458	0.00539647	365.180
1980N	0.00435635	0.00401258	103.058	2005cf	0.00748518	0.00603148	435.808
1981D	0.00435635	0.00384896	152.112	2003du	0.00807892	0.00764223	130.918
2006dd	0.00435635	0.00461021	-76.105	2009ig	0.00845251	0.00702938	426.644
2007on	0.00435635	0.00463160	-82.518				

Table 1. Peculiar velocities of the 27 SN Ia and host-galaxies, respectively.

Peculiar velocities with a positive sign mean that the SN Ia is moving away from us as observer in addition to the pure Hubble flow. Velocities with negative sign show that the SN Ia is moving locally in the direction of observer.

These peculiar velocities are only the right ones if the absolute magnitude <M> of the SN Ia used is real valid.

4.5.3 Real redshift distances of SN Ia

After we could correct the redshifts of the SN Ia we can calculate all real redshift distances of these cosmic objects. Table 2 shows the result.

SN Ia	R_{ea}	R_{ee}	R_{0e}	R_{0a}	D_e	D_0	D
2011fe	2,584.50	2,580.45	2,582.88	2,586.94	4.05	4.06	6.49
1989B	2,582.42	2,574.92	2,579.42	2,586.94	7.51	7.52	12.02
1998bu	2,582.73	2,575.72	2,579.92	2,586.94	7.01	7.02	11.22
2001el	2,579.30	2,566.61	2,574.21	2,586.94	12.69	12.73	20.32
1981B	2,581.31	2,571.94	2,577.55	2,586.94	9.37	9.39	15.00
1990N	2,578.09	2,563.39	2,572.18	2,586.94	14.70	14.75	23.55
1994D	2,580.99	2,571.09	2,577.02	2,586.94	9.90	9.92	15.85

2012cg	2,581.10	2,571.38	2,577.20	2,586.94	9.72	9.74	15.56
2015F	2,578.94	2,565.66	2,573.61	2,586.94	13.29	13.33	21.28
2012fr	2,580.01	2,568.49	2,575.39	2,586.94	11.52	11.55	18.45
1980N	2,580.04	2,568.57	2,575.44	2,586.94	11.47	11.50	18.37
1981D	2,580.32	2,569.32	2,575.91	2,586.94	11.00	11.03	17.62
2006dd	**2,579.02**	**2,565.85**	**2,573.73**	**2,586.94**	**13.17**	**13.21**	**21.09**
2007on	2,578.98	2,565.75	2,573.67	2,586.94	13.23	13.27	21.18
2011iv	2,580.20	2,568.99	2,575.70	2,586.94	11.21	11.24	17.95
1998aq	2,578.72	2,565.06	2,573.23	2,586.94	13.66	13.70	21.88
2011by	2,578.05	2,563.28	2,572.12	2,586.94	14.77	14.82	23.66
2013dy	2,579.55	2,567.26	2,574.61	2,586.94	12.29	12.32	19.68
2012ht	2,577.93	2,562.95	2,571.91	2,586.94	14.98	15.03	23.99
1994ae	2,576.68	2,559.65	2,569.84	2,586.94	17.03	17.10	27.29
2007sr	2,579.30	2,566.61	2,574.21	2,586.94	12.69	12.73	20.32
2002fk	2,574.66	2,554.28	2,566.46	2,586.94	20.38	20.48	32.66
1995al	2,576.30	2,558.62	2,569.19	2,586.94	17.67	17.75	28.31
2007af	2,577.67	2,562.28	2,571.49	2,586.94	15.40	15.45	24.66
2005cf	2,576.59	2,559.40	2,569.68	2,586.94	17.19	17.26	27.54
2003du	2,573.84	2,552.10	2,565.09	2,586.94	21.74	21.85	34.83
2009ig	2,574.89	2,554.88	2,566.83	2,586.94	20.01	20.10	32.06

Table 2. Redshift distance D and the further redshift distances D_i and R_{jk} of all 27 SN Ia.

To interpret the distances from Table 2:

For a more detailed explanation, we take into account the SN Ia **2006dd** (**bold** market within the table), for example, and use it to interpret the meaning of the distances shown in the table.

The "light-travel time" always means the time interval between the emission of light (the time at that time $t_{e,2006dd}$) by the SN Ia 2006dd and today (t_0), i.e. $\Delta t_{2006dd} = t_0 - t_{e,2006dd}$. This light-travel time is generally different for all observable cosmic objects, here especially formal noticed for the individual SN Ia 2006dd we will consider.

a) The today's (t_0) distance between the selected SN Ia 2006dd and us as observers is $D_0 \approx 13.21$ Mpc.

b) The distance at that time (t_e) between this SN Ia 2006dd and us as observers was $D_e \approx 13.17$ Mpc.

According to this, the distance between the two participated cosmic objects has increased by about 0.04 Mpc during the light-travel time $\Delta t_{2006dd} = t_0 - t_{e,2006dd}$.

c) The SN Ia 2006dd has been shifted expansively away from the origin of the coordinates by $\Delta R_e = R_{0e} - R_{ee} \approx$ 7.88 Mpc during the light-travel time due to the time-dependent scale parameter a(t).

d) The galaxy with us as observers has been expansively shifted away from the origin of the coordinates by $\Delta R_a = R_{0a} - R_{ea} \approx 7.92$ Mpc during the light-travel time due to a(t).

The difference between the two displacement distances is of course the increase in the distances between the two participated cosmic objects noted above.

e) The real light path (redshift distance) covered by the photons within the interval of time $\Delta t_{2006dd} = t_0 - t_{e,2006dd}$ is $D \approx 21.09$ Mpc. It is unequal to the other mentioned distances D_i and greater than these, because of small redshifts for SN Ia used.

These redshift distances are only the right ones if the absolute magnitude <M> of the SN Ia used is real valid.

4.6 Evaluation of the data from the black hole in M87

For the sake of simplicity, we summarize the data taken from the specialist literature on the galaxy M87 containing a black hole (BH) in it in the first line of Table 3 {see [5] and [6]}.
The second line lists the data specified in this paper, which usually differ from those in the specialist literature.

	D [Mpc]	**M_B [mag]**	**z**	**m_B [mag]**	**Θ_{BH} [µas]**	**$\delta/2 = R_S$ [pc]**	**M_{BH} [g]**
literature	16.9 / 16.8	-23.5	0.004283	9.6	42		1.2928E+43
we	19.60	-26.86				1.49843E-03	1.5571E+43

Table 3. Summary of data from galaxy M87 containing a black hole in it.

The theory was adapted to the measured angle size Θ_{BH} given in the specialist literature. Overall, a larger redshift distance D, a bigger absolute magnitude M_B and a similar value of mass M_{BH} of the black hole follow.

Table 4 lists the values found by means of our theory for all redshift distances R_{jk}, D_i and D, respectively.

[Mpc]	R_{ea}	R_{ee}	R_{0e}	R_{0a}	D_e	D_0	**D**
we	2,579.58	2,567.34	2,574.67	2,586.94	12.24	12.27	19.60
literature	---	---	---	---	---	---	16.8/16.9

Table 4. Redshift distances D_i, D and R_{jk} belonging to the black hole in M87.

From these values, the expansion-related shifts in distance of the galaxy M87 and of the galaxy with us as observers can be calculated, which took place during the time of light travel.

The theory from the specialist literature does not know the most distances listed in Table 4. Therefore, they cannot be calculated using this theory and not determined in terms of value.

The distance D differs because of the physical meaning: In our theory, D is the real physical light path, which is not the case in the astrophysical specialist literature.

We briefly interpret the meaning of the distances listed in Table 4, whereby the light-travel time is again defined as described in a former chapter:
a) The today's (t_0) distance between the BH or the galaxy M87 and us as observers is $D_0 \approx 12.27$ Mpc.
b) The distance at that time (t_e) between the BH (or M87) and us as observers was $D_e \approx 12.24$ Mpc.
Accordingly, the distance between the two cosmic objects has increased by about 0.03 Mpc during the light-travel time $\Delta t_{BH,\,M87} = t_0 - t_{e,BH,\,M87}$.

c) The BH (or M87) has been shifted expansively away from the origin of the coordinates by $\Delta R_e = R_{0e} - R_{ee} \approx$ 7.33 Mpc during the light-travel time due to the time-dependent scale parameter a(t).

d) The galaxy with us as observer was expansively shifted away from the origin of the coordinates by $\Delta R_a = R_{0a} - R_{ea} \approx 7.36$ Mpc during the light-travel time due to a(t).

e) The real light path (redshift distance) covered by the photons during the interval of time $\Delta t_{BH,\ M87} = t_0 - t_{e,BH,\ M87}$ is $D \approx 19.60$ Mpc. It is unequal to the other mentioned distances D_i and greater than these.

4.7 Maximum values known today: Galaxy UDFj-39546284 and Quasar J0313

The galaxy UDFj-39546284 [8] currently holds the record among the galaxies with a redshift of z = 10.3, while the quasar J0313 [7] with z = 7.642 holds the analog record among the quasars.

Table 5 summarizes all calculated redshift distances of the two cosmic objects.

object name	z	R_{ea}	R_{ee}	R_{0e}	R_{0a}	D_e	D_0	D	object
J0313	7.642	614.29	-435.17	-1,832.60	2,586.94	1,049.46	4,419.54	3,022.11	quasar
UDFj-39546284	10.3	513.73	-435.26	-2,191.80	2,586.94	948.99	4,778.74	3,022.20	galaxy

Table 5. All calculated redshift distances R_{jk}, D_i and D for the two cosmic objects with the maximum redshifts and for us as observer [Mpc].

We see some negative redshift distances:
Here $R_e(t) = a(t)r_e < 0$ is valid what means $r_e < 0$ in these cases. Both observed cosmic objects were beyond of the origin of coordinates at the time t_e. In addition, negative distances of both objects are bigger today.

Table 6 summarizes the spatial shifts of the objects with respect to the origin of coordinates due to the expansion during the associated light travel times.

object name	$R_{0e} - R_{ee}$	$R_{0a} - R_{ea}$	object
J0313	-1,397.43	1,972.64	quasar
UDFj-39546284	-1,756.54	2,073.21	galaxy

Table 6. Expansion-related shifts in the distances of the quasar and the galaxy and of the observer [Mpc].

We have already explained above how the tables have to be interpreted.

Fig. 14 shows the distances D_i and D of the three special astrophysical objects chosen to analyze in this paper in one diagram, whereby we have entered all numerical values for the distances in Mpc.

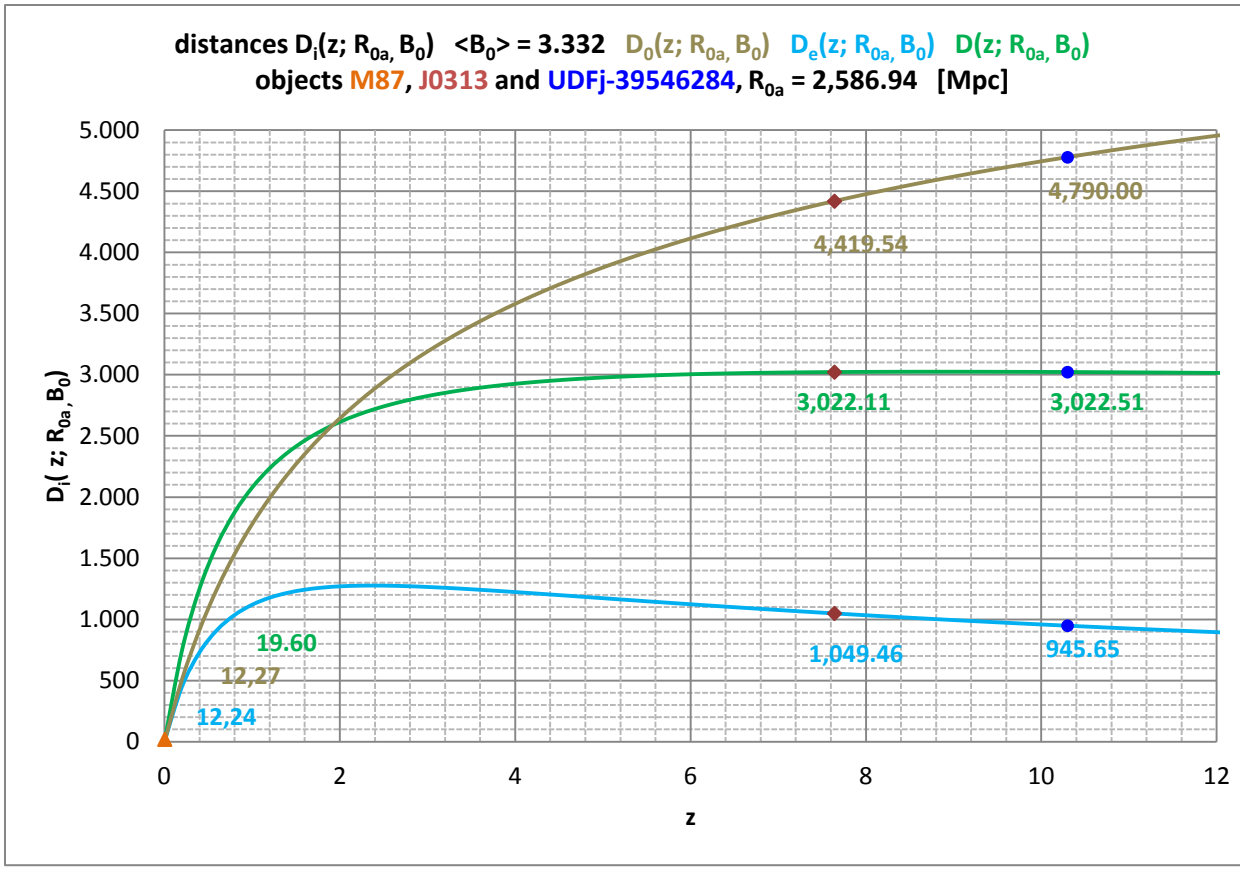

Figure 14. All distances D_i and D for M87, J0313 and UDFj-39546284.

We recognize that from about z ≈ 2 the today's distance D_0 is larger than the associated light path D. Furthermore, we see that the light path distance D is hardly growing anymore for larger redshifts from about z ≈ 6. Therefore, the difference between D_{quasar} and D_{galaxy} are very small although the difference of both redshifts is relatively large.

5 About the mass of Friedman sphere

The cause of the expansion of the universe is its effective constant mass M_{Fs} or the time-varying matter density ρ(t), respectively. It ensures that the scale parameter a(t) changes over time. To check this statement, one should simply set the matter density in the Friedmann equation to zero.

Every cosmologist, therefore, has to ask himself where exactly this mass is located within the universe. He can gain an answer for this by borrowing the appropriate ideas from classical non-relativistic Newtonian cosmology. There he has to imagine a mass sphere whose radius changes over time (e.g. grows). This means that the mass in question is completely within this sphere, and it is evenly distributed and remains there according to the cosmological principle.

In relativistic cosmology, the time depend product of scale parameter and co-moving coordinate distance R(t) = a(t)r takes over the role of the physical radius of the mass sphere, and it holds that the entire mass to be considered is inside this sphere (Friedmann sphere named here).

The Fig. 15 shows the projection of a Friedmann sphere in to the plane at time t_0 (today) in which examples of possible places for an observer and galaxy observed are drawn.

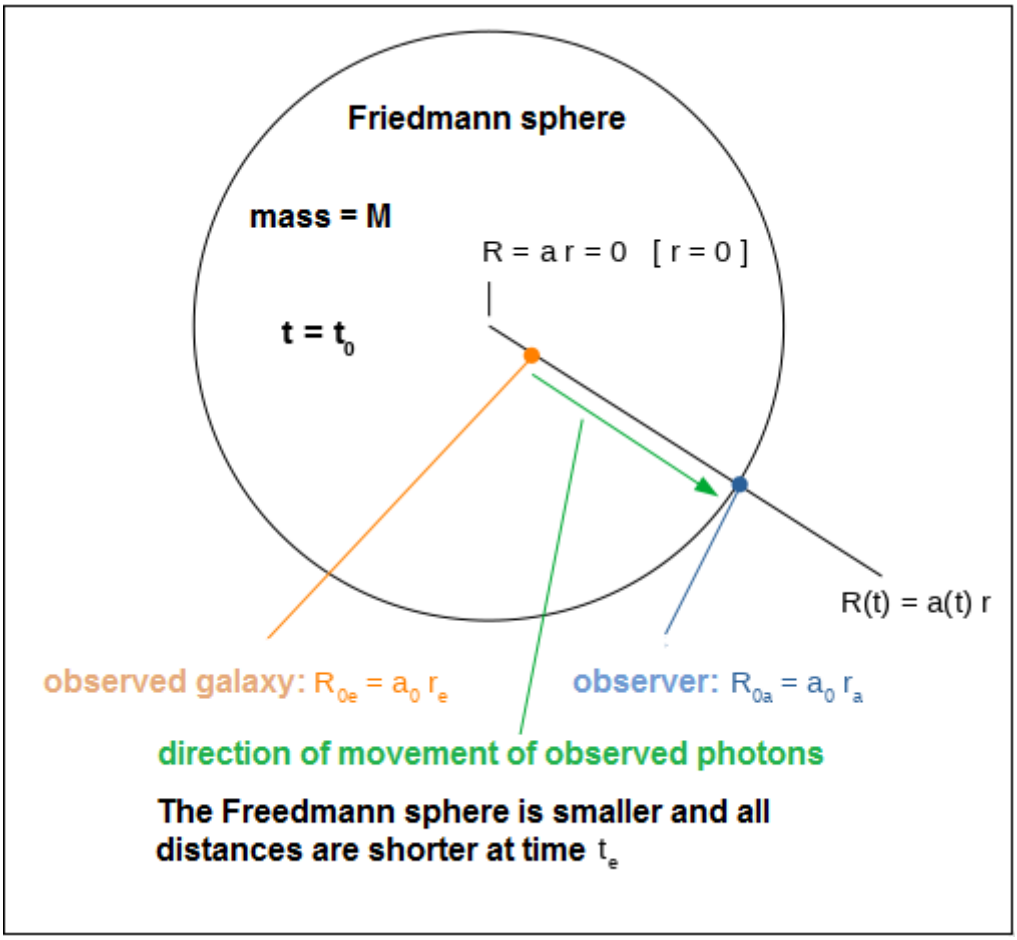

Figure 15. Friedmann sphere containing examples of physical locations of an observer and a galaxy.

Because of the law of conservation of mass

$$M_{Fs} = \frac{4\pi}{3}\rho_0 {a_0}^3 {r_a}^3 = \frac{4\pi}{3}\rho_0 {R_{0a}}^3 \tag{66}$$

which is used here, we see that R_{0a} is today's radius of the Friedmann sphere with today's mass density ρ_0.

Of course, each observer can also, e.g., look in exactly the opposite direction to the direction shown (green arrow). In this case, he looks again into a Friedmann sphere, which belongs to this direction. The observer can of

course also look in any other directions. The observer always looks into Friedmann spheres, which of course partially overlap.

A universe thought to be spherical corresponds to at least one sphere with the radius 2 x R_{0a}, since beyond R_{0a} there is always also mass.
Every observer sits on the surface of Friedmann spheres. Nevertheless, he can believe that his place is also in a center of such a Friedmann sphere.

If we would put the position of an observer a little outside the Friedmann sphere shown in Fig. 15, he would find the same situation as described above, if the universe would be actually much larger than a sphere with the radius 2 x R_{0a} or even infinitely large.

Hint:
Because of possible negative distances R_{ee} and R_{0e} an observable galaxy can have also co-moving coordinates with $r_e < 0$. Such cosmic objects are on the other side of the center of the Friedmann sphere with r = 0.

6. Hubble parameter again

At this point we explicitly point out that our equation of today's Hubble parameter - which also only applies to very small redshifts - differs significantly from the definition (!) used in the specialist literature. The equations for both are

$$H_{0a}(R_{0a}, B_0) \approx \frac{3}{(B_0+2)}\frac{c_0}{R_{0a}} \qquad (we)$$
$$and \qquad (67)$$
$$H_{0,lit} = \frac{\dot{a}_0}{a_0} \qquad (literature) \quad .$$

For an arbitrary point in time t this reads

$$H_a(t) \approx \frac{3}{[B(t)+2]}\frac{c_0}{a(t)r_a} \qquad (we)$$
because of
$$B(t) = \frac{1}{2}\sqrt{\frac{R_S}{R_a(t)}} = \frac{1}{2}\sqrt{\frac{R_S}{a(t)r_a}} \quad being \quad \frac{c_0}{r_a} = const \quad \frac{R_S}{r_a} = const \quad R_S = const \qquad (67a)$$
and

$$H_{lit}(t) = \frac{\dot{a}(t)}{a(t)} \qquad (literature) \quad .$$

The index a generally indicates the spatial proximity to the observer, meaning r = r_a.

In our theory, the numerator contains the constant physical speed of light c_0 in vacuum, while the current, i.e. the variable spatial expansion speed da/dt is found at this place in the specialist literature.

In the more recent past - time t_x - our distance from the origin of coordinates $R_{xa} < R_{0a}$ was slightly smaller than the current one and the Hubble parameter H_{xa} was therefore correspondingly larger (also via the parameter B_x).

Furthermore, in the case of the Hubble parameter in specialist literature, the non-physical spatial expansion speed da/dt can have been arbitrarily large in the past and, in addition, the scale parameter a(t) arbitrarily small. Both types of Hubble parameters therefore show a completely different physical behavior!

In addition, our Hubble parameter is actually made up of physical quantities, while the Hubble parameter in the astrophysical literature is only defined using the non-physical scale parameter a(t), although to the latter can be assigned a suitable unit of measurement - e.g. Mpc. This means that a(t) alone per se is not a physical distance. This meaning only applies to the real physical distance R(t) = a(t)r and the differences that can be calculated from it.

The Hubble parameter is the proportionality factor between the so called Hubble speed $V = c_0 z$ and a distance, i.e. the actual linear Hubble law applies

$$\begin{aligned} & V = c_0 z = H_{0a} D \approx \frac{3}{(B_0 + 2)} \frac{c_0}{R_{0a}} D \qquad (we) \\ & and \\ & V_{lit} = c_0 z = H_{0,lit} D_{lit} = \frac{\dot{a}_0}{a_0} D_{lit} \qquad (literature) \quad . \end{aligned} \tag{68}$$

For the redshift z it simply follows therefore

$$\begin{aligned} & z = \frac{H_{0a}}{c_0} D \approx \frac{3}{(B_0 + 2)} \frac{D}{R_{0a}} \qquad (we) \\ & and \\ & z = \frac{H_{0,lit}}{c_0} D_{lit} = \frac{\dot{a}_0}{c_0} \frac{D_{lit}}{a_0} \qquad (literature) \quad . \end{aligned} \tag{69}$$

In the specialist literature, the redshift z is therefore depending on the ratio of the current speed da/dt to the speed of light c_0 in the product with the ratio of an object distance D_{lit} and the current scale parameter a_0.

Our redshift, on the other hand, is depending on the ratio of the light path distance D and the current distance R_{0a} of the observer galaxy from an origin of the coordinates and is besides proportional to the factor that contains the parameter B_0.

Using the parameter B_0

$$B_0 = 2\sqrt{\frac{R_{0a}}{R_S}} \qquad with \qquad R_S = \frac{2GM_{Fs}}{{c_0}^2} \tag{33b}$$

we see in our case

$$z = \frac{H_{0a}}{c_0} D \approx \frac{3}{2\left(\sqrt{\frac{R_{0a}}{R_S}} + 1\right)} \frac{D}{R_{0a}} \quad , \tag{70}$$

i.e. an direct dependence on the Schwarzschild radius R_S, or more precisely on the ratio R_{0a} to R_S.

Overall, it is somewhat unclear in the specialist literature what exactly corresponds to the distance D_{lit}.

Fig. 16 shows the difference between our non-approximated redshift distance D and the linear Hubble redshift distance that is an approximated one.

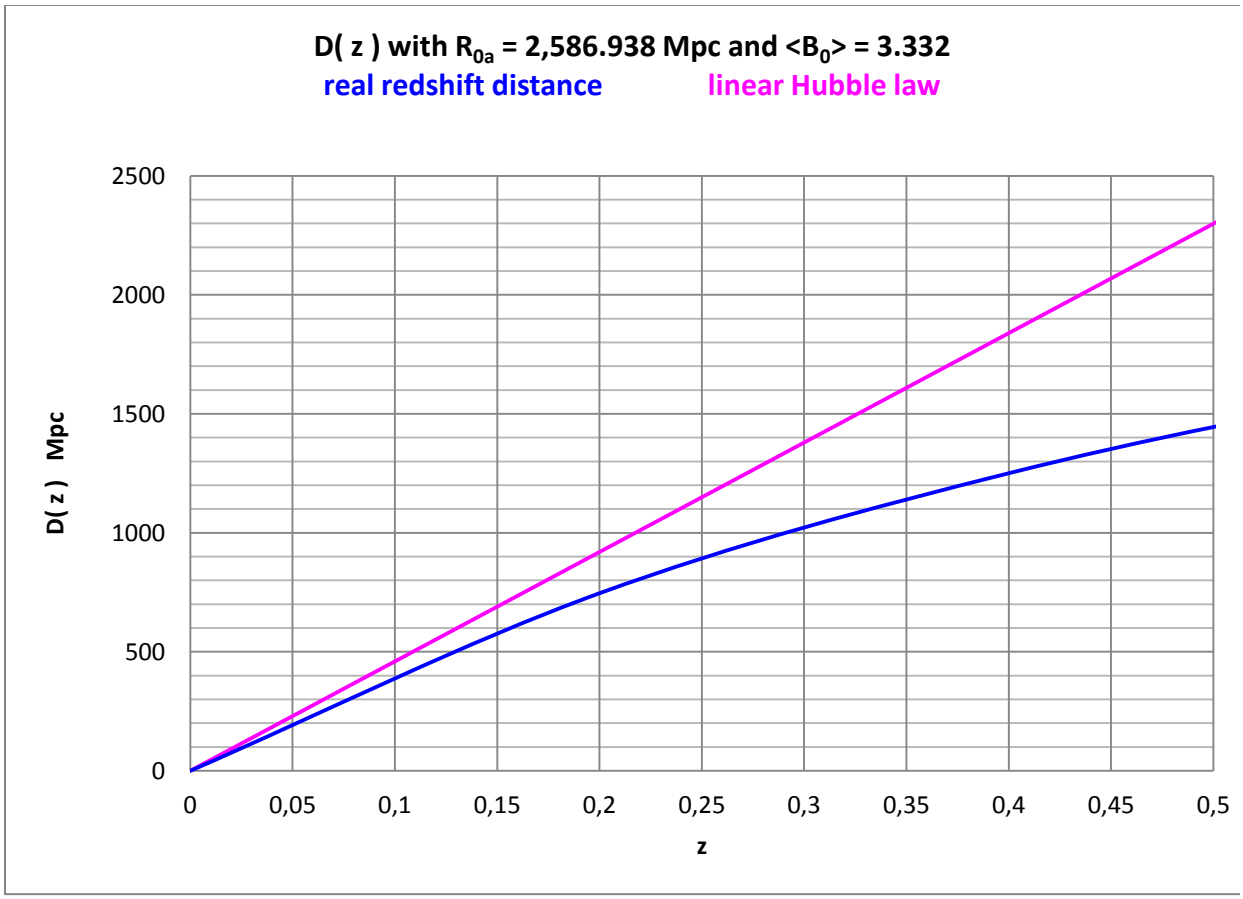

Figure 16. Non-approximated redshift distance D compared to the linear Hubble redshift distance.

It can be seen that the two curves already clearly separate from each other at $z \approx 0.0075$, and that Hubble's linear law results in distances that are significantly too large for larger redshifts, so that it is no longer applicable from around this value.

Recall:
Of course, it should be noted that the Hubble parameter H_{0a} in our theory results from an approximation for small redshifts z. This is not the case in specialist literature.

Because the value of R_{0a} could be identified, we can use it in Eq. (67) and get

$$H_{0,lit} = \frac{\dot{a}_0 r_a}{a_0 r_a} = \frac{\dot{R}_{0a}}{R_{0a}} \qquad or \qquad \dot{R}_{0a} = H_{0,lit} R_{0a} \qquad (literature) \tag{71a,b}$$

if we supplement simple with r_a.

Hint:
In the specialist literature of cosmology the redshift distance is calculated using regular $r_a = 0$. This is not the case in our theory!

If we replace $H_{0a,lit}$ using Eq. (8)

$$H_{0,lit} = \sqrt{\frac{2GM_{Fs}}{a_0^{\,3} r_a^{\,3}}} = \sqrt{\frac{2GM_{Fs}}{R_{0a}^{\,3}}} = c_0 \sqrt{\frac{R_S}{R_{0a}}} \frac{1}{R_{0a}} \qquad (literature) \tag{8a}$$

we get

$$\dot{R}_a(t) = c_0 \sqrt{\frac{R_S}{R_a(t)}} \qquad (literature) \quad . \tag{71c}$$

In this form we see that dR(t)/dt was infinitely big at t = 0 because R(t) was infinitely small at this time. This means that dR(t)/dt becomes smaller with time.

Because $H_{0,lit} = 69.557$ is also known for us [Eq. (8)], we find $dR_a/dt = 179{,}938.38$ km/s for today. This is the today's physical velocity of expansion, which is valid for all observers (homogeneity of the cosmological model).

In summary, we find two different Hubble times:

$t_{H\_0,lit}$ = 14.07 x 10^9 years and t_{H_0a} = 15.01 x 10^9 years, respectively.

7. Concluding remarks

The real light path D(z) of the photons through the expanding universe corresponds to a dynamic distance and appear therefore as an apparent one. This distance is not identical to the today's distance $D_0(z)$ between the cosmic objects.
For every conceivable observer, the cosmic objects are not radial-spatially, where they appear at first glance!
In cosmology, nothing is what it seems to be if we look at distances and therefore in the past.

Of course, all cosmological relevant astrophysical objects have a today's distance $D_0(z)$. However, this is not observable, but we can calculate it. Photons that are emitted at this distance from the observed galaxy cannot have reached us so far.

A fundamental property of quantum mechanics is that it can only make probability statements about the microscopic objects it deals with. Here we see that both the measuring and the theorizing astrophysics and cosmology, respectively, strictly speaking, can only make statements about mean values of very distant and large numbers of cosmic objects (see e.g. the magnitude - redshift relation of quasars).
This may be one of the reasons why both theories - the theory for the extremely small and the theory for the extremely large - do not fit together, i.e. cannot be brought together.

Note of thanks:
I would like to thank my wife for the long-standing toleration and the corresponding endurance of my almost constant virtual absence. What would I be without her?!

8. Appendices

8.1 Equations

We use the following equations to solve the EFE with the help of the modified FLRWM.

a) mFLRWM

$$ds^2 = \frac{a_0}{a_e} {c_0}^2 dt^2 - a^2(t) dr^2 - a^2(t) r^2 \left(d\vartheta^2 + \sin^2 \vartheta \, d\varphi^2 \right) \tag{3a}$$

a_e is the scale parameter at the time of emission of the observed photons.

b) Christoffel symbols

$$\Gamma^{\sigma}_{\lambda\mu} = \frac{g^{\sigma\nu}}{2} \left(\frac{\partial g_{\mu\nu}}{\partial x^{\lambda}} + \frac{\partial g_{\lambda\nu}}{\partial x^{\mu}} - \frac{\partial g_{\mu\lambda}}{\partial x^{\nu}} \right) \tag{A1}$$

Using the mFLRWM (3a) the calculated Christoffel symbols result in

$$\Gamma^0_{00} = -\frac{1}{2} \frac{1}{c_0} \frac{\dot{a}}{a} \qquad \Gamma^0_{11} = \frac{1}{c_0} \frac{a^2 \dot{a}}{a_0} \qquad \Gamma^0_{22} = \frac{1}{c_0} r^2 \frac{a^2 \dot{a}}{a_0} \qquad \Gamma^0_{33} = \frac{1}{c_0} r^2 \sin^2 \vartheta \frac{a^2 \dot{a}}{a_0} \tag{A2}$$

and

$$\Gamma^1_{01} = \Gamma^1_{10} = \frac{1}{c_0} \frac{\dot{a}}{a} \qquad \Gamma^1_{22} = -r \qquad \Gamma^1_{33} = -\sin^2 \vartheta r \tag{A3}$$

and

$$\Gamma^2_{02} = \Gamma^2_{20} = \frac{1}{c_0} \frac{\dot{a}}{a} \qquad \Gamma^2_{12} = \Gamma^2_{21} = \frac{1}{r} \qquad \Gamma^2_{33} = -\sin\vartheta \cos\vartheta \tag{A4}$$

and

$$\Gamma^3_{03} = \Gamma^3_{30} = \frac{1}{c_0} \frac{\dot{a}}{a} \qquad \Gamma^3_{13} = \Gamma^3_{31} = \frac{1}{r} \qquad \Gamma^3_{23} = \Gamma^3_{32} = \cot\vartheta \quad . \tag{A }$$

c) Ricci tensor $R_{\mu\nu}$

$$R_{\mu\nu} = \partial_{\alpha} \Gamma^{\alpha}_{\mu\nu} - \partial_{\nu} \Gamma^{\alpha}_{\mu\alpha} + \Gamma^{\alpha}_{\alpha\lambda} \Gamma^{\lambda}_{\mu\nu} - \Gamma^{\alpha}_{\nu\lambda} \Gamma^{\lambda}_{\mu\alpha} \tag{A6}$$

Using the calculated Christoffel symbols the components of the Ricci tensor - the left sides of EFE - result in

$$R_{00} = -\frac{3}{{c_0}^2} \left(\frac{\ddot{a}}{a} + \frac{1}{2} \frac{\dot{a}^2}{a^2} \right) \tag{A7}$$

and

$$R_{11} = \frac{1}{c_0^{\,2}} \frac{a}{a_0} \left(a\,\ddot{a} + \frac{5}{2}\dot{a}^2 \right) \tag{A8}$$

and

$$R_{22} = \frac{1}{c_0^{\,2}} r^2 \frac{a}{a_0} \left(a\,\ddot{a} + \frac{5}{2}\dot{a}^2 \right) \tag{A9}$$

and

$$R_{33} = \frac{1}{c_0^{\,2}} r^2 \sin^2 \vartheta \frac{a}{a_0} \left(a\,\ddot{a} + \frac{5}{2}\dot{a}^2 \right) \quad . \tag{A10}$$

All other components of $R_{\mu\nu}$ are equal to zero.

d) energy-momentum tensor $T_{\mu\nu}$

For solving the Einstein equations, we need furthermore the components of the energy-momentum tensor $T_{\mu\nu}$:

$$T_{\mu\nu} = \left[\left(\rho + \frac{P}{c_0^{\,2}} \right) u_\mu u_\nu - P\, g_{\mu\nu} \right] \quad . \tag{A11}$$

P describes the possible pressure within the universe and ρ stand for the energy and matter density, respectively. The four covariant components of the four-velocity u_μ read in our case

$$u_\mu = \left(\sqrt{\frac{a_0}{a}} c_0, 0, 0, 0 \right) \quad , \tag{A12}$$

because all space components are equal to zero (co-moving coordinates).
Therefore, we get

$$T_{\mu\nu} = \begin{pmatrix} \frac{a_0}{a}\rho c_0^{\,2} + \left(1 - \frac{a_0}{a}\right)P & 0 & 0 & 0 \\ 0 & Pa^2 & 0 & 0 \\ 0 & 0 & Pa^2 r^2 & 0 \\ 0 & 0 & 0 & Pa^2 r^2 \sin^2\vartheta \end{pmatrix} \quad . \tag{A13}$$

e) Trace of energy-momentum tensor

The trace T of the energy-momentum tensor results in

$$T = \rho c_0^{\,2} + \left(\frac{a}{a_0} - 4\right)P \quad . \tag{A14}$$

f) concrete EFE

Putting all together, we find at first

$$\begin{aligned} R_{00} &= \frac{4\pi G}{c_0^{\,4}}\left[\frac{a_0}{a}\rho c_0^{\,2} + \left(1 + 2\frac{a_0}{a}\right)P\right] && (a) \\ R_{11} &= \frac{4\pi G}{c_0^{\,4}}a^2\left[\rho c_0^{\,2} + \left(\frac{a}{a_0} - 2\right)P\right] && (b) \\ R_{22} &= \frac{4\pi G}{c_0^{\,4}}a^2 r^2\left[\rho c_0^{\,2} + \left(\frac{a}{a_0} - 2\right)P\right] && (c) \\ R_{33} &= \frac{4\pi G}{c_0^{\,4}}a^2 r^2 \sin^2\vartheta\left[\rho c_0^{\,2} + \left(\frac{a}{a_0} - 2\right)P\right] && (d) \quad . \end{aligned} \tag{A15}$$

Combining this with the left sides of EFE calculated above we get

$$\begin{aligned} -\frac{3}{c_0^{\,2}}\left(\frac{\ddot{a}}{a} + \frac{1}{2}\frac{\dot{a}^2}{a^2}\right) &= \frac{4\pi G}{c_0^{\,4}}\left[\frac{a_0}{a}\rho c_0^{\,2} + \left(1 + 2\frac{a_0}{a}\right)P\right] && (e) \\ \frac{1}{c_0^{\,2}}\frac{a}{a_0}\left(a\ddot{a} + \frac{5}{2}\dot{a}^2\right) &= \frac{4\pi G}{c_0^{\,4}}a^2\left[\rho c_0^{\,2} + \left(\frac{a}{a_0} - 2\right)P\right] && (f) \\ \frac{1}{c_0^{\,2}}r^2\frac{a}{a_0}\left(a\ddot{a} + \frac{5}{2}\dot{a}^2\right) &= \frac{4\pi G}{c_0^{\,4}}a^2 r^2\left[\rho c_0^{\,2} + \left(\frac{a}{a_0} - 2\right)P\right] && (g) \\ \frac{1}{c_0^{\,2}}r^2\sin^2\vartheta\frac{a}{a_0}\left(a\ddot{a} + \frac{5}{2}\dot{a}^2\right) &= \frac{4\pi G}{c_0^{\,4}}a^2 r^2\sin^2\vartheta\left[\rho c_0^{\,2} + \left(\frac{a}{a_0} - 2\right)P\right] && (h) \end{aligned} \tag{A16}$$

or

$$\frac{\ddot{a}}{a}+\frac{1}{2}\frac{\dot{a}^2}{a^2}=-\frac{4\pi G}{3c_0{}^2}\left[\frac{a_0}{a}\rho c_0{}^2+\left(1+2\frac{a_0}{a}\right)P\right] \qquad (e')$$

$$a\ddot{a}+\frac{5}{2}\dot{a}^2=\frac{4\pi G}{c_0{}^2}a\,a_0\left[\rho c_0{}^2+\left(\frac{a}{a_0}-2\right)P\right] \qquad (f') \qquad \text{(A17)}$$

$$a\ddot{a}+\frac{5}{2}\dot{a}^2=\frac{4\pi G}{c_0{}^2}a\,a_0\left[\rho c_0{}^2+\left(\frac{a}{a_0}-2\right)P\right] \qquad (g')$$

$$a\ddot{a}+\frac{5}{2}\dot{a}^2=\frac{4\pi G}{c_0{}^2}a\,a_0\left[\rho c_0{}^2+\left(\frac{a}{a_0}-2\right)P\right] \qquad (h') \quad .$$

g) Friedmann equations

In summary, we get only two remaining different Friedmann equations, which read

$$\frac{\ddot{a}}{a}+\frac{1}{2}\frac{\dot{a}^2}{a^2}=-\frac{4\pi G}{3}\frac{a_0}{a}\rho \qquad (I)$$

$$\frac{\ddot{a}}{a}+\frac{5}{2}\frac{\dot{a}^2}{a^2}=4\pi G\,\frac{a_0}{a}\rho \qquad (II) \quad , \qquad \text{(A18)}$$

if we neglect the possible pressure P.

These both equations together lead to the wanted main Friedmann equation

$$\left(\frac{\dot{a}}{a}\right)^2=\frac{8\pi G}{3}\,\frac{a_0}{a}\rho \quad , \qquad \text{(A19)}$$

which describes the evolution of the scale parameter a(t) in time.

During this evolution of the universe, the mass M_{Fs}, which is represented by the mass density ρ, is a constant:

$$M_{Fs}=\frac{4\pi}{3}\rho(t)a^3(t)r_a{}^3=const=\frac{4\pi}{3}\rho(t_0)a^3(t_0)r_a{}^3$$

$$or \qquad \text{(A20)}$$

$$\rho=\frac{3}{4\pi}\frac{M_{Fs}}{a^3\,r_a{}^3} \quad .$$

Therefore, the main Friedmann equation takes the form

$$\dot{a}=\sqrt{\frac{2GM_{Fs}a_0}{r_a{}^3}}\,\frac{1}{a} \quad . \qquad \text{(A21)}$$

The square root has a constant value.

8.2 Tables

In this table appendix, we provide the essential data that we have used and some of the data that we have edited or generated for general purposes.

$< V >_i$	$< z >_i$	$< V >_i$	$< z >_i$	$< V >_i$	$< z >_i$
17.12072194	0.269543711	19.5118161	1.28508799	19.7439932	1.86740102
18.42994924	0.434725324	19.4960406	1.30997857	19.7431839	1.90379949
18.77986464	0.514410603	19.5406994	1.33635871	19.73815	1.91629442
18.92177101	0.571495206	19.5648675	1.36044896	19.7370051	1.94113536
19.01993232	0.621120135	19.5526283	1.38646193	19.6390299	1.96661139
19.07454597	0.665043993	19.5667343	1.41249746	19.7247377	1.99498872
19.10685279	0.710045685	19.5917766	1.43823632	19.7073435	2.02761873
19.20756345	0.750830795	19.5835759	1.46348111	19.7225437	2.05895826
19.23878173	0.788362662	19.6146701	1.4877084	19.7209927	2.09067964
19.34673999	0.823077834	19.6560914	1.50872984	19.7166723	2.12286464
19.35605189	0.857111675	19.6421545	1.53039989	19.7562211	2.15726452
19.35379019	0.889902425	19.6730062	1.55031021	19.6955838	2.1915251
19.35354202	0.925268472	19.669718	1.57141117	19.7102256	2.23148844
19.36111675	0.958962211	19.691489	1.59370615	19.6203328	2.27565595
19.36687535	0.99085674	19.6689622	1.61663057	19.6516638	2.32895262
19.39208122	1.021072758	19.7130344	1.64024196	19.7034969	2.39616356
19.41216018	1.049862944	19.7208742	1.66227637	19.6915454	2.47184715
19.43737733	1.076128596	19.7568415	1.68460462	19.7660462	2.57089058
19.47736041	1.10186802	19.6973942	1.70912747	19.7708009	2.71401918
19.4307727	1.129618161	19.7453187	1.7323057	19.7781162	2.90122279
19.45345178	1.157690919	19.7723632	1.75403384	19.9208291	3.05796277
19.4499718	1.18469656	19.7568754	1.77625888	20.0279357	3.20401523
19.50609701	1.208890017	19.7599436	1.79742358	20.2283362	3.40521263
19.48940778	1.233098139	19.7587704	1.82113988	20.5549521	3.7254264
19.47597857	1.259028765	19.7435195	1.84394303	21.3169261	4.34427862

Table 1. Mean values from the quasar data set used according to [1].

Hint:

$<z>_i$ (with i = 1, 2, ..., 75) are the 75 mean values of the redshifts of the quasars in the redshift intervals formed.

$<V>_i$ are the associated 75 mean values of the apparent visual magnitude of the quasars.

z_i (end of interval)	N_i	z_i (end of interval)	N_i
0.24669	622	3.45369	128,884
0.49338	3,891	3.70038	130,205
0.74008	12,827	3.94708	131,357
0.98677	25,495	4.19377	132,019
1.23346	41,724	4.44046	132,432
1.48015	58,818	4.68715	132,669
1.72685	78,456	4.93385	132,848
1.97354	97,109	5.18054	132,902
2.22023	110,358	5.42723	132,924
2.46692	117,810	5.67392	132,932
2.71362	121,463	5.92062	132,949
2.96031	123,820	6.16731	132,972
3.20700	126,835	6.41400	132,977

Table 2. Numbers N_i summed up in the redshift intervals z_i of the quasars according to [1].

SN Ia	μ_{TRGB}	μ_{Ceph}	μ or $<\mu>$	m_{CSP_B0}	m_{SC_B}	m_B or $<m_B>$	M_i or $<M_i>$	V_{NED}	z
1980N	31.46		31.46	12.08		12.08	-19.38	1,306.00	0.004356347
1981B	30.96	30.91	**30.94**	11.64	11.62	**11.63**	**-19.31**	1,050.00	0.003502423
1981D	31.46		31.46	11.99		11.99	-19.47	1,306.00	0.004356347
1989B	30.22		30.22	11.16		11.16	-19.06	689.00	0.002298257
1990N		31.53	31.53	12.62	12.42	**12.52**	**-19.01**	1,050.00	0.003502423
1994D	31.00		31.00	11.76		11.76	-19.24	1,050.00	0.003502423
1994ae	32.27	32.07	**32.17**	12.94	12.92	**12.93**	**-19.24**	1,552.00	0.005176915
1995al	32.22	32.50	**32.36**	13.02	12.97	**13.00**	**-19.37**	1,886.00	0.006291019
1998aq		31.74	31.74	12.46	12.24	**12.35**	**-19.39**	1,368.00	0.004563157
1998bu	30.31		30.31	11.01		11.01	-19.30	689.00	0.002298257
2001el	31.32	31.31	**31.32**	12.30	12.20	**12.25**	**-19.07**	1,047.00	0.003492416
2002fk	32.50	32.52	**32.51**	13.33	13.20	**13.27**	**-19.25**	1,864.00	0.006217635
2003du		32.92	32.92	13.47	13.47	**13.47**	**-19.45**	2,422.00	0.008078922
2005cf		32.26	32.26	12.96	13.01	**12.99**	**-19.28**	2,244.00	0.007485178
2006dd	31.46		31.46	12.38		12.38	-19.08	1,306.00	0.004356347
2007af	31.82	31.79	**31.81**	12.72	12.70	**12.71**	**-19.10**	1,983.00	0.006614576
2007on	31.42		31.42	12.39		12.39	-19.03	1,306.00	0.004356347
2007sr	31.68	31.29	**31.49**	12.30	12.24	**12.27**	**-19.22**	1,702.00	0.005677261
2009ig		32.50	32.50	13.29	13.46	**13.38**	**-19.13**	2,534.00	0.008452514
2011by		31.59	31.59	12.63	12.49	**12.56**	**-19.03**	1,368.00	0.004563157
2011fe	29.08	29.14	**29.11**	9.82	9.75	**9.79**	**-19.33**	455.00	0.001517717

2011iv	31.42		31.42	12.03		12.03	-19.39	1,306.00	0.004356347
2012cg	31.00	31.08	**31.04**	11.72	11.55	**11.64**	**-19.41**	1,050.00	0.003502423
2012fr	31.36	31.31	**31.34**	12.09	11.92	**12.01**	**-19.33**	1,302.00	0.004343005
2012ht		31.91	31.91	12.66	12.70	**12.68**	**-19.23**	1,447.00	0.004826672
2013dy		31.50	31.50	12.23	12.31	**12.27**	**-19.23**	1,410.00	0.004703254
2015F		31.51	31.51	12.40	12.28	**12.34**	**-19.17**	1,271.00	0.0042396
						<M>=	**-19.24**		

Table 3. Summary of the data which we have used from the 27 SN Ia according to [3].

SN Ia values that can be traced back to a mean value are marked in green (**bold**).
The individual meanings of the data can be found in the original article mentioned.

The data for the angular-size redshift diagram can be found in full in [2].

References

[1] M.-P. Véron-Cetty and P. Véron, A Catalogue of Quasars and Active Nuclei, 13th edition, March 2010, http://www.obs-hp.fr/catalogues/veron2_13/veron2_13.html

[2] K. Nilsson, M. J. Valtonen, J. Kotilainen and T. Jaakkola, Astro. J. 413 (1993), 453.

[3] W. L. Freedman u. a., The Carnegie-Chicago Hubble Program. VIII. An Independent Determination of the Hubble Constant Based on the Tip of the Red Giant Branch, arXiv.org:1907.05922

[4] The Planck Collaboration: Planck 2018 results. VI. Cosmological parameters, arXiv:1807.06209

[5] The Event Horizon Telescope Collaboration, The Astrophysical Journal Letters, 875:L1 (17pp), 2019 April 10, https://doi.org/10.3847/2041-8213/ab0ec7

[6] de.wikipedia.org/wiki/Messier_87, retrieved 18.12.2021

[7] de.wikipedia.org/wiki/Quasar, retrieved 18.12.2021

[8] de.wikipedia.org/wiki/UDFj-39546284, retrieved 18.12.2021

[9] G. Dautcourt, Was sind Quasare?, S. 68, Abb. 18, BSB B.G. Teubner Verlagsgesellschaft, 4. Auflage 1987

[10] A. Sandage, R. G. Kron, and M. S. Longair, The Deep Universe, Springer-Verlag, 1995, (Saas-Fee Advanced Course 23, Lecture Notes 1993, Swiss Society for Astrophysics and Astronomy, Publishers: B. Binggeli and R. Buser).

[11] St. Haase, New derivation of redshift distance without using power expansions, Fundamental Journal of Modern Physics, Volume 17, Issue 1, 2022, Pages 1-40
This paper is available online at http://www.frdint.com/

[12] Haase S. 2023. Redshift distances in flat Friedmann-Lemaître-Robertson-Walker spacetime. PREPRINTS:RU. https://doi.org/10.24108/preprints-311.2484
